A STUDY OF THE PROCESS AND CAUSES OF

Aβ(25-35) AMYLOID FORMATION

A Dissertation

by

KATHERINE VALE RIDINGER

Submitted to the Office of Graduate Studies of
Texas A&M University
in partial fulfillment of the requirements for the degree of

DOCTOR OF PHILOSOPHY

December 2009

Major Subject: Biochemistry

A STUDY OF THE PROCESS AND CAUSES OF

Aβ(25-35) AMYLOID FORMATION

A Dissertation

by

KATHERINE VALE RIDINGER

Submitted to the Office of Graduate Studies of
Texas A&M University
in partial fulfillment of the requirements for the degree of

DOCTOR OF PHILOSOPHY

Approved by:

Chair of Committee,	John Martin Scholtz
Committee Members,	Carlos Nick Pace
	Michael Polymenis
	Allison Ficht
Head of Department,	Gregory Reinhart

December 2009

Major Subject: Biochemistry

ABSTRACT

A Study of the Process and Causes of Aβ(25-35) Amyloid Formation. (December 2009)

Katherine Vale Ridinger, B.S., Angelo State University

Chair of Advisory Committee: Dr. John Martin Scholtz

Amyloid fibrils results from a type of ordered polypeptide aggregation that is associated with ailments such as Alzheimer's disease (AD). Annually, millions of people in the United States alone develop and die from AD. Therefore, it is necessary to understand not only the process of amyloid formation, but also the causes of this specific type of aggregation. This study used Aβ(25-35) since it is a fragment of the Alzheimer's peptide that behaves like the full length peptide found in patients with AD.

To study the process of amyloid formation, several methods were used so that a more complete picture of the stepped aggregation process could be realized. Several oligomeric species were detected and described many of which could not have been observed without using the complete battery of methods utilized here. The oligomeric species detected included a novel 'rolled sheet' that appeared to be the immediate precursor of amyloid fibrils, and two supermolecular species that appear after amyloid fibrils were formed.

In determining the causes of amyloid formation, two significant discoveries were made. First, by partial sequence randomization, truncation, and Ala scanning mutagenesis, the critical amyloidogenic region of Aβ(25-35) was found to be residues 30-35. This critical core region is important because it is thought to be the region that initiates amyloid formation, therefore knowing the residues involved in the region is a useful tool for developing methods of fibril formation prevention. Second, by inserting all naturally occurring amino acids into position 34 of Aβ(25-35), three distinct classes of variants were observed and the effect of several physiochemical properties on amyloidosis were examined. Hydrophobicity, solubility, and β-strand propensity were found to affect aggregation to the greatest extent. Also within these two studies, our results suggest that early oligomers are the cytotoxic species as opposed to amyloid fibrils or other larger macromolecular assemblies.

DEDICATION

To my mother,

who always encouraged me to try, and who taught me that

anything worth having was worth working for

ACKNOWLEDGEMENTS

I would like to thank my committee chair, Dr. Scholtz, for supporting me and giving me the opportunity to work on this project. I would also like to thank Dr. Pace for his encouragement and advice, as well as the other members of my committee: Dr. Ficht and Dr. Polymenis, for their guidance and support throughout the course of this research.

Thanks also go to my labmates, friends, and colleagues. Also to the faculty and staff of Molecular and Cellular Medicine and Biochemistry & Biophysics for all the help they have given. Special thanks to Dr. Yun Wei for helping me all throughout this study, and to Dr. Saul Trevino for his advice and motivation.

Finally, thanks to my mother for always being there for me and inspiring me to continue my education.

NOMENCLATURE

Aβ	Amyloid beta peptide
AD	Alzheimer's disease
DLS	Dynamic light scattering
DMA	Disappearance of monomer assay
EM	Electron microscopy
ThT	Thioflavin T

TABLE OF CONTENTS

CHAPTER Page

LIST OF FIGURES

FIGURE Page

LIST OF TABLES

CHAPTER I

INTRODUCTION

In 1907, Alois Alzheimer reported a patient with the first recorded instance of what would later be called Alzheimer's disease (AD).[1] Over the next several years, more cases were reported until AD became a recognized form of dementia and is now the sixth leading cause of death in the United States.[2] One of the hallmarks of AD is the presence of a substance that Alzheimer found in his first deceased patient's brain. This substance had originally been studied by Virchow in 1854, and termed 'amyloid' since it reacted to iodine like starch.[3] It was over a century later, in the mid-1980s, that the substance that Alzheimer described, now termed amyloid plaques, was finally discovered to be primarily made up of a polypeptide called Aβ(1-42).[4]

Aβ(1-42) is a peptide that is the product of the incorrect cleavage of the amyloid precursor protein (APP). Specifically, APP is a membrane protein that, when properly cleaved by α- and γ-secretases, is perfectly harmless because the α-secretase cleavage site is in the middle of Aβ(1-42).[4] However, if APP is cleaved by β- and γ-secretases, Aβ(1-42) is formed, released, and able to aggregate (Fig. 1).[4] It is important to note here that Aβ(1-42) is not the only peptide that is involved in Alzheimer's disease. There is a great deal of debate within the "Alzheimer's field" concerning the relative importance of

---

This dissertation follows the style of *Journal of Molecular Biology*.

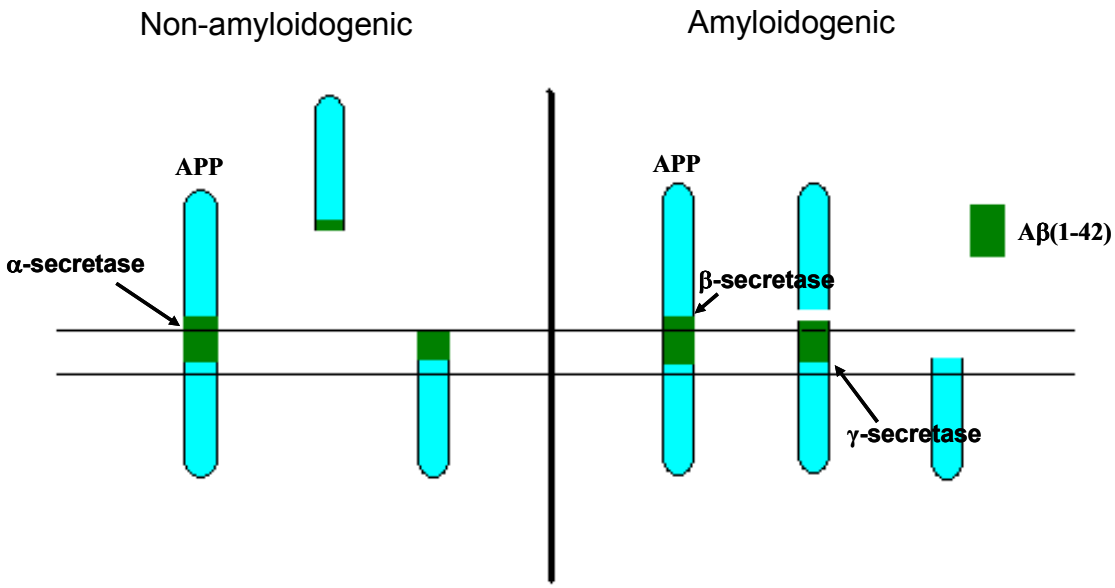

Figure 1. Amyloid precursor protein (APP) cleavage and production of Aβ(1-42). α- β- and γ-secretases are proteolytic enzymes with different specificities. α-secretase cleaves between Lys16 and Leu17. β-secretase cleaves between Tyr10 and Glu11. γ-secretase cleaves at multiple sites within the transmembrane domain. The cleavage of APP by β- and γ-secretases releases the Aβ(1-42).

Tau, a microtubule-associated protein, and Aβ(1-42) in the disease.[5] Despite the controversy, aggregation of Aβ(1-42) certainly appears to start the disease process, which could cause Tau to aggregate and cause cell death. [4-6] This initial importance of Aβ(1-42) in AD has been shown a number of ways. Naturally occurring mutations of APP that result in familial early onset Alzheimer's are prevalent, suggesting that the mutations that affect the production of Aβ(1-42) greatly influence AD.[7-11] Also, patients with Down Syndrome, characterized by trisomy of chromosome 21, are much more likely to develop AD early in life since the gene for APP is located on chromosome 21.[12; 13] Several studies on the effects of adding Aβ(1-42) or segments of Aβ(1-42) have resulted in cognitive deficiencies and cell toxicity, though the mechanism of cell death is still unclear.[6; 14-20] One thing seems certain: the appearance of amyloid plaques made up of Aβ(1-42) is a diagnostic hallmark, if not the direct cause of the disease.[21]

A popular hypothesis of cytoxicity is that an oligomeric form of the peptide in the early stages of Aβ(1-42) amyloid formation is responsible, either directly or indirectly, for disease symptoms and cell death. [14; 17; 21-27] Therefore, it is necessary to not only understand why the aggregation takes place, but also how to prevent it. To achieve this, several species found in the process of aggregation from the monomeric peptide to the amyloid fibrils were tested to determine which causes cell death and neurodegeneration. This is a difficult undertaking since the oligomers along the pathway of fibrillation are transient, heterogeneous, and difficult to isolate. However, there is some evidence that

dimers cause toxicity,[14] although it is more likely that a larger, yet still soluble oligomer is the culprit.[17; 21-27]

Considerable work has been devoted to investigating other aspects of fibrillation using variants or mutants. One of the most useful tools for studying some properties of proteins is to mutate specific residues and measure differences in the properties between the mutant and the wild-type protein. Since this procedure is efficient and effective, the same principle has been applied to studying various aspects of amyloid formation. Amyloidogenic peptides and proteins have been altered to determine the stability of fibrils,[8; 28-32] elucidate the kinetics or rates of aggregation,[8; 32-36] establish the properties of amyloid propensity,[28; 32] discover critical regions of the peptide for fibrillogenesis,[29-31; 37] and discern which physiochemical properties have the largest influence on amyloid formation.[33; 36; 38-43]

Specifically, an understanding of the physiochemical properties that are responsible for amyloid formation is an important and open question. Several properties have been implicated in various studies conducted over the past decade, ranging from the more popular culprit of hydrophobicity to the lesser accused solubility.[33; 34; 36; 39-41; 44-53] The data from these studies have been incorporated into the few algorithms that attempt to predict amyloid formation using only the sequence, and in some cases, the solution conditions.[45; 48; 52; 54] Despite the considerable amount of work invested in answering the question of which properties dictate fibrillation, there is still no clear consensus.

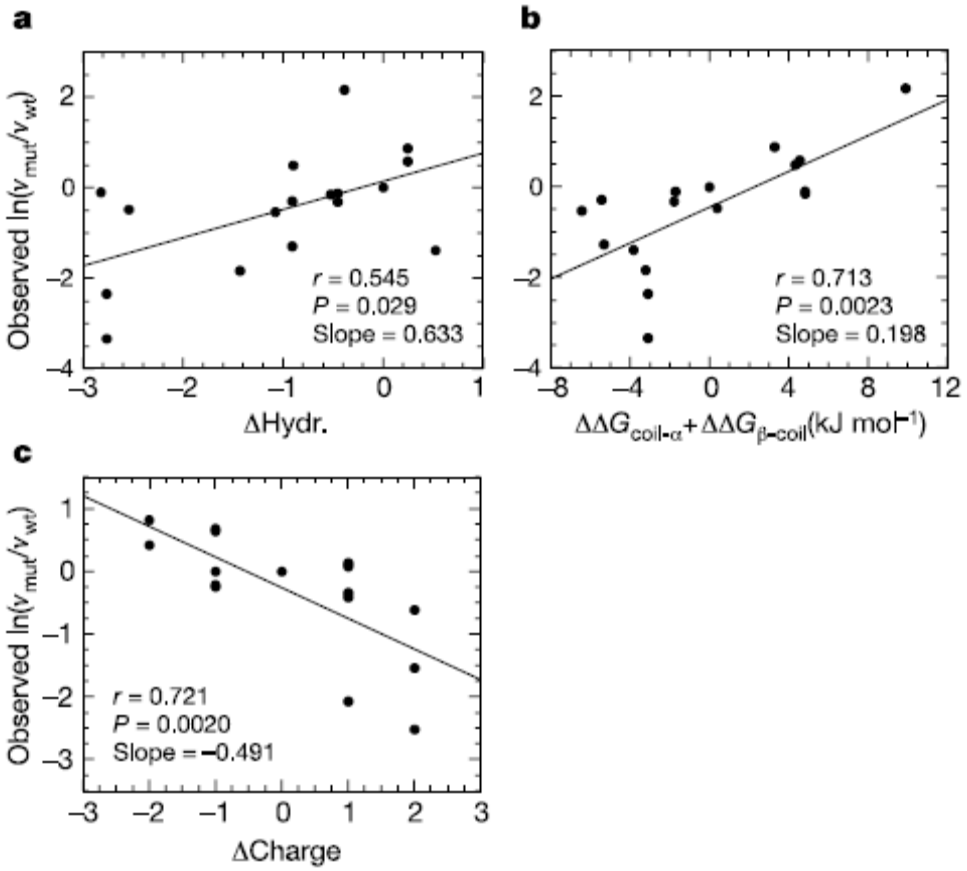

Figure 2. Correlation values between the aggregation rate and physiochemical properties.[45] The change in aggregation rate of mutant protein (ν_{mut}) from wild-type (ν_{wt}) was plotted against change in (a.) hydrophobicity, (b.) the propensity to convert from α-helical to β-strand conformation, and (c.) change in charge.

In Figure 2, we show the correlation values between several of these physiochemical properties and thermodynamic (critical concentration) and kinetic (half-time) parameters from a study using Leu34 mutants of Aβ(25-35), an amyloidogenic fragment of Aβ(1-42). These two parameters are useful for determining the propensity of peptides to form fibrils and are discussed further in Chapter II. Critical concentration (C_r) is the concentration of monomeric peptide still in solution when an equilibrium is established between the monomeric peptide and amyloid fibrils, and therefore this parameter can demonstrate the extent of amyloid formation.[55] C_r can be used to find the fibril stability (ΔG) by the equation[8]:

$$\Delta G = -RT\ln(1/C_r) \quad (1)$$

Therefore, fibril stability is reflective of the extent of amyloid formation of a mutant peptide in relation to the wild-type peptide. C_r can also be used to find the half-time ($t_{1/2}$), which is the amount of time necessary for the monomeric concentration to be halfway between the initial concentration and the C_r. This parameter can indicate the kinetics of aggregation, which is useful in comparisons between peptides.

To further understand the influence of the various physiochemical properties, the stability of fibrils formed from variants of Aβ(1-40) and Aβ(1-42) have been collected (Table 1) and will be discussed below. The different physiochemical properties

Table 1. Amyloid formation in Aβ(1-40) and Aβ(1-42) variants

Mutant[a]	ΔΔG[b]	Mutant	ΔΔG[b]	Mutant	ΔΔG[b]	Mutant	ΔΔG[b]
Naturally occuring[d]		*Ala scanning*[f]		*Cys scanning*[g]		*Pro scanning*[h]	
A2T	-0.3	F4A	-0.4	F4C	0.2	F4P	-0.8
H6R	-0.2	H13A	0.6	H6C	0.2	H6P	0.1
D7N	-0.3	H14A	0.3	H13C	1	G9P	0.3
A21G	0.4	Q15A	0.8	K16C	0.4	V12P	0.5
E22G	0	K16A	1.2	L17C	2	H14P	-0.2
E22K	-0.5	L17A	1.1	V18C	1.9	G15P	1.4
E22Q	-0.9	V18A	1.3	F19C	1.2	K16P	1.3
D23N	-0.3	F19A	1.5	F20C	0.5	L17P	1.5
Position 18[c,e]		F20A	0.8	A21C	1.6	V18P	2.8
V18A	0.5	E22A	0.1	E22C	1.9	F19P	3.2
V18D	1.3	V24A	1.4	D23C	0	F20P	3.2
V18E	0.7	G25A	0.8	V24C	1.5	A21P	1.2
V18F	-0.1	S26A	0.3	G25C	1.5	E22P	-0.3
V18G	0	N27A	1	S26C	0.8	D23P	-0.3
V18H	0.5	K28A	0.9	N27C	1.5	V24P	1.4
V18I	-0.6	G29A	-0.1	K28C	0.9	G25P	2.1
V18K	1.3	I31A	2	G29C	1.5	S26P	1.6
V18L	0	I32A	1	A30C	0.7	N27P	0.8
V18N	0.4	G33A	0.5	I31C	1.5	K28P	0.9
V18P	1.1	L34A	1.2	I32C	2.2	G29P	0.5
V18Q	0	M35A	1.1	G33C	0.4	A30P	0.1
V18R	0.3	V36A	1	L34C	1.7	I31P	2.1
V18S	1.1	G37A	0.8	M35C	1.9	I32P	2.2
V18T	0.2	G38A	0.7	V36C	1.7	G33P	1.8
V18W	-0.1	V39A	0.3	G38C	0.9	L34P	1.5
V18Y	-0.7	V40A	0.4			M35P	0.8
						V36P	1
						G37P	0.4
						G38P	0.6
						V39P	0.4

[a] Aβ(1-40): DAEFRHDSGYEVHHQKLVFFAEDVGSNKGAIIGLMVGGVV.

[b] Values expressed in kcal/mol. ΔG_{wt} =-6.4 kcal/mol

[c] ΔG calculated by $\Delta G=-RT\ln(1/c_r)$. $\Delta\Delta G=\Delta G_{mutant} - \Delta G_{wt.}$ Positive value indicates less "stable fibrils".

[d]Data taken from Ref. 7. [e]Data taken from Ref. 27. [f]Data taken from Ref 28.

[g]Data taken from Ref 29. [h]Data taken from Ref. 30

implicated in amyloid formation are discussed in greater detail below. The focus is on mutations to segments of or full length Aβ(1-42) and the resulting changes in fibril stability (Table 1) or the kinetics of amyloid formation, although studies conducted in other model peptides or proteins are mentioned for comparison.

Hydrophobicity

The physiochemical property of a polypeptide that is most often considered to have the largest effect on fibril formation is hydrophobicity.[32-34; 39; 40; 42; 43; 49] At first glance, this makes sense as the hydrophobicity will determine whether a peptide is more likely to interact with an aqueous solvent or with itself. If the peptide is composed of several hydrophobic groups such as Ile, Leu, and Phe, logically, it should be significantly more likely to aggregate in some fashion, although not necessarily to amyloid fibrils. To further demonstrate this idea, consider the amino acids Asn and Ser compared to Ile, Phe, or Leu. Asn and Ser are both hydrophilic, and it has been shown that mutating either of these amino acids to a more hydrophobic amino acid will encourage aggregation (Table 1).[28; 32; 43; 48; 56] In contrast, the more hydrophobic amino acids such as Ile, Phe, and Leu have a much higher propensity to form amyloid fibrils when insertd into an amyloidogenic peptide (Table 1). [28; 32; 35; 39; 40; 48; 56] One amino acid that does not follow this trend very well is hydrophilic Gln that is shown to be capable of forming amyloid in previous studies.[28; 57] Gln repeats are also associated with Parkinson's disease, demonstrating that it is a hydrophilic amino acid that, at least in continuous repeats, forms fibrils.[57]

Solubility

A property of an amino acid that is similar to hydrophobicity is solubility, and due to how closely the two are related, it is very difficult to study these two properties separately, perhaps more so than hydrophobicity and any other physiochemical property. Solubility should have an effect on amyloid formation based on the same arguments used for hydrophobicity: how the peptide interacts with the solution as compared to itself should predetermine aggregation propensity. Despite the similarity in hydrophobicity to solubility, the latter is often overlooked in favor of the former,[50; 52] and in only one instance is solubility considered to significantly contribute to amyloidosis.[50]

Because the hydrophobicity and solubility of a residue are so complementary, examples that alter fibril formation would, overall, be the same between these two properties. However, there are some instances where they can be distinguished; the most telling is when comparing Gln and Ser. The physiochemical properties of these two amino acids are all comparable, except for solubility, where Ser is found to be significantly more soluble than Gln.[58] Therefore, a large difference in the propensity of these two amino acids to form amyloid can be attributed to the change in solubility. Because Ser is much more soluble, and is also much less likely to form amyloid, we can say with a fair degree of certainty that the solubility is to blame for reduced fibril formation when Ser is substituted for Gln in various peptides.[28; 32; 48]

β-strand propensity

Secondary structure propensity of a residue has been implicated as a factor in amyloid formation. However, only β-strand propensity is addressed here because it is more commonly considered important since the basic structure of a fibril is β-sheet conformation.[34; 39; 41; 42; 45; 48; 51; 52; 59-61] Logically, an increase in the β-strand propensity of a peptide should increase the probability of that peptide to form amyloid fibrils, and this has been shown to be true.[36; 41; 56; 61] Conversely, introducing amino acids with a low propensity for β-strand formation discourages fibril formation, most likely due to the probability of the mutated amino acid disrupting the β-strand structure.[30]

Two amino acids that are known to disrupt β-strand structure are Pro and Gly, both of which have been shown to be poor amyloid forming amino acids (Table 1).[28; 32; 39; 43; 48] The amino acids that have a high β-strand propensity (i.e. Phe, Tyr, and Ile) are among the top amyloid formers,[40] however, there is difficulty determining whether the ability to form fibrils is due to β-strand propensity, hydrophobicity, or solubility since many of the amino acids that are likely to form β-strand are also hydrophobic and show less solubility, and all three of these physiochemical properties should encourage amyloid formation.

Electrostatic interactions

Introducing charged amino acids into a peptide can have a substantial inhibitory effect on amyloid formation, and has therefore been one of the prevalent contenders in

determining fibrillation.[33; 44; 49; 53; 62] Replacement of hydrophobic, low solubility residues like Val or Ile with charged amino acids such as Glu, Lys, or Arg has been shown to significantly reduce fibril formation (Table 1).[32; 42] However, there are instances where charge encourages aggregation due to electrostatic attraction between oppositely charged residues like Glu and Lys, [41] which is similar to what we found in our studies of Aβ(25-35) (Chapter V). Both of these instances make sense as they relate back to the basic properties of electrostatic interactions where like charges repel and opposite charges attract. It is also logical that the introduction of a single positive charge to an already positively charged peptide inhibits aggregation, while the addition of a negative charge to the same peptide would be more likely to encourage peptide-peptide interactions and possibly amyloid formation.

Glu and Lys have several physiochemical properties in common, suggesting that the two might show similar amyloid formation tendencies, and this has been shown to be the case in one study.[48] However, other studies utilizing different host peptides demonstrate Glu as being significantly more likely to form fibrils than Lys.[28; 32] This disagreement is seen when comparing all of the charged amino acids. Most likely, the dissention is due to the context of each amino acid in question and any charge-charge interactions between the amino acid and neighboring residues.

Aromaticity

Like hydrophobicity, it is difficult to differentiate the effects of aromaticity from other

physiochemical properties of peptides, i.e. hydrophobicity, solubility, and β-strand propensity since amino acids that are aromatic are hydrophobic, low on the solubility scale, and are likely to form β-strands. However, aromatic residues are, on occasion, implicated for increasing amyloid formation due to stabilizing π-π stacking.[38; 63; 64] In a majority of the studies that proclaim aromaticity of the peptide promotes fibril formation, it is more the result of noticing the prevalence of aromatic residues in amyloidogenic peptides than a strategic mutational analysis to test the effect of introducing aromatic side groups.[63; 64] Another study that examined the importance of aromatic groups mutated from Phe and Tyr groups in acylphosphatase[38] and β2-microglobulin[65] and found in most cases, the rates of aggregation decreased. However, the mutations that removed aromaticity also changed all of the physiochemical properties known to affect amyloid formation, making the effect of residue aromaticity on aggregation hard to determine. It is possible that aromatic groups could play a role in fibril formation as three of the amino acids that have been shown to encourage aggregation are aromatic (Phe, Tyr, and Trp).[28; 32; 39] However, the other physiochemical properties of these three amino acids are also favorable for amyloidosis. Therefore, unfortunately, there is not enough data right now to state whether this is a true correlation or due to the other physiochemical properties of the aromatic amino acids.

Methionine oxidation

Much of the focus thus far has been on the physiochemical properties of amino acids that have been shown to have a noticeable effect on amyloid formation, however there are

other factors that should be mentioned when discussing fibrilogenesis. Over the years, oxidation of Met to Met-sulfoxide has been found to be increasingly important in aggregation of various peptides and subsequent neurodegeneration.[66-68] Of particular interest, Met35 in Aβ has been frequently studied to determine the importance of the oxidation state on amyloid formation, although other peptides and proteins with oxidizable groups have been examined also. Oxidizing Met has been found, in many cases, to inhibit aggregation or cytotoxicity, typically in Aβ.[66-70] The common consensus as to why oxidation of Met inhibits aggregation is the alteration of the interactions between the oxidized Met and surrounding residues, specifically, electronic and hydrophobic interactions.[66; 68; 69]

Oxidation, however, is rarely included in the prediction of fibrillation due to the rarity of Met as well as the importance of Met placement within the peptide.[66] Due to this, oxidation is often overlooked in favor of the more prevalent physiochemical properties that have been shown to have a consistent, and more independent of context, effect on aggregation. Again, there is the possibility that the change in oxidation state changes a more prominent physiochemical property, i.e. hydrophobicity, and it is the change in hydrophobicity rather than oxidation that affects aggregation.

Sequence

In a variety of proteins and peptides, it has been shown that more than just the composition of amino acids is important: that the sequence of the residues has a large

effect on amyloid formation.[71; 72] This is usually attributed to the patterning of the amino acids, primarily alternating polar and nonpolar residues that easily gives rise to β-strand structure due to the 2 residue periodicity of a β-strand.[73-76] Since amyloid fibrils are in a β-strand conformation, any pattern that increases the probability of forming β-strand also increases the probability of forming fibrils. This has been demonstrated with *de novo* peptides that have the alternating polar/nonpolar pattern that were able to form fibrils.[75; 76] That study found that the periodicity of amino acids dictated the secondary structure assumed, as opposed to the propensity of the amino acids used. This shows that even though the individual amino acid composition is important, the sequence, or context for mutated residues, can be equally as crucial for fibril formation.

Solution conditions

Solution conditions must also be taken into account when studying amyloid formation, since they certainly have an effect on the structure, rate, and extent of aggregation.[61; 77-88] The most obvious of these is temperature.[81; 82; 86; 88] Temperature is complicated because it can have a significant effect on amyloidosis by influencing a variety of physiochemical properties. However, temperature can also destabilize any structure a protein or peptide may have, which should allow aggregation. Another prominent variable that affects amyloid formation is pH, which in some cases inhibitory and in others, promoting.[61; 84; 87; 88] What is difficult about determining the importance of pH is that it directly affects charge, and therefore also the hydrophobicity and solubility, leaving the actual root of the amyloid formation unknown. Also, in order to predict

whether pH will adversely affect fibril formation depends on the pI of the peptide.[50] As the pH approaches the pI, aggregation increases. Salt concentration has also been shown to affect amyloidosis since the salt ions can screen the charges on the peptide and promote aggregation.[49; 77] In addition to charge screening, salts such as GuHCl, can denature any peptide or protein structure, which also has been shown to encourage fibrillation, presumably by destabilizing the structure and allowing non-native interactions.[88]

A point of contention in literature is the importance of agitation versus quiescent conditions during incubation. Agitation is often discussed as a possible promoter of fibril formation since keeping the solution in motion should allow the peptide to interact and aggregate, therefore lowering the time needed for aggregation.[78; 79; 82; 88] Although, it has also been suggested that quiescent conditions are more conducive to stable amyloid fibrils.[78] In this debate at least, it appears that the goals of each experiment should dictate whether agitation or quiescence is more appropriate.

Prediction methods

Thus far, the various properties and factors have been discussed; however they have not been described in context of the various prediction methods. There have been several attempts to predict amyloid formation from sequence considerations alone. Each method is unique, though there are common physiochemical properties between them.

To demonstrate the variety of prediction methods, two will be examined that have been reported to predict amyloidogenic regions of a peptide.

Dobson and coworkers[48] define the propensity of a peptide to aggregate, P_{agg}, as:

$$P_{agg} = \alpha_{hydro} I^{hydro} + \alpha_{\alpha} I^{\alpha} + \alpha_{\beta} I^{\beta} + \alpha_{pat} I^{pat} + \alpha_{ch} I^{ch} \qquad (2)$$

I^{hydro} is the additive hydrophobicity of each residue in the sequence with a range of -4 for Arg to +2.3 for Phe.[89] I^{α} is the combined α-helical propensity of the sequence and has a range of -0.4 for Leu to +0.6 for Cys; the values for Gly and Pro were set by Dobson, *et.al.* as 2 and 1.5, respectively.[48; 90] I^{β} is the pooled β-strand propensity of the sequence with a range of -0.8 for Ile to +1.7 for Gln; the Pro value was also set by Dobson, *et.al.* at 0.1.[48; 90] The collective values calculated for I^{hydro}, I^{α}, and I^{β} were all normalized to the length of the sequence. I^{pat} is the patterning of hydrophobic residues and is calculated by adding +1 for each region of five consecutive alternating hydrophobic/hydrophilic residues in the sequence.[48; 73] Finally, I^{ch} is the absolute value of the net charge of the peptide.[48] The coefficients for hydrophobicity, patterning, and β-strand propensity demonstrate that these factors encourage amyloid formation. However, the opposite is true of the α-helical propensity and net charge coefficients, two physiochemical properties that are commonly shown to inhibit amyloid formation. The coefficients range from -1.99 for hydrophobicity to +5.0 for β-strand propensity, showing that each of the properties contributes differently to amyloid formation. The

two properties that have the smallest coefficient are charge and patterning, signifying that these are thought to have a nominal effect on aggregation.

Caflisch and coworkers have taken a different approach to the aggregation-prone regions of a peptide.[52] In their method the aggregation propensity is calculated using aromaticity, β-strand propensity, charge, solubility, accessible surface area, and several other properties. As opposed to the Dobson's method, this more complicated approach expresses the perceived importance of each property by its placement in several levels of algorithms. Specifically, the solubility and accessible surface area minimally add to aggregation, while aromaticity, β-strand propensity, and charge are thought to have a much larger effect.

TANGO[59; 91] is a program that attempts to predict β-aggregation, which certainly could be the same as amyloid fibrils, though, is not necessarily so. This program uses several of the same physiochemical properties as the Dobson and Caflisch algorithms, i.e. hydrophobicity, electrostatics, and β-sheet propensity; however, TANGO adds in something new: hydrogen bonding. Hydrogen bonding is not commonly assumed to have an effect on aggregation, although inclusion of hydrogen bonding into the TANGO program increased the correlation value, suggesting that perhaps it should not be overlooked.

Another prediction program is Waltz from Switch laboratory.[92; 93] It is clear that Waltz takes into account similar physiochemical properties as the aforementioned methods; unfortunately, the specific properties and weights are not described, and therefore cannot be discussed here.

Each of these models emphasizes different properties that are believed to be crucial to amyloidosis, though there are some commonalities. For example, at least three of the methods take β-strand propensity and charge into account, implying that these two physiochemical properties are believed to be important for fibril formation, which is supported by the literature surveyed earlier. However, where Dobson, *et.al.* examine the effect of hydrophobicity, α-helical propensity, and hydrophobic patterning, Caflisch, *et.al.* look at aromaticity, solubility, and accessible surface area and TANGO accounts for hydrogen bonding. Several of these properties are not as well supported in literature, and therefore are more open to speculation as to their importance to fibril formation. Despite the differences in these methods, all are able to predict amyloid formation with a fair degree of accuracy, though none are ideal, which demonstrates that further studies must be done to determine the effect of each property to construct a more accurate prediction method.

Conclusions

It is clear that the physiochemical properties of the polypeptide that influence amyloid formation are still not well understood, in part because so many of the properties are

closely related. To further highlight how little is known, we see that not only is the composition important for amyloidosis, but the context of each residue appears to have an effect. Despite how difficult it is to distinguish between the various physiochemical properties, it is possible, and therefore a relative importance of each property is achievable given careful, deliberate studies using an assortment of proteins and peptides to ensure that residue context is taken into account.

CHAPTER II

MATERIALS AND METHODS

Peptide synthesis reagents and FPLC/HPLC buffer materials were procured from Advanced Chemtech (Louisville, KY), Aldrich, (St. Louis, MO), and Fisher Scientific (Pittsburgh, PA). Filters used for FPLC/HPLC solutions and buffers were purchased from Millipore (Ireland). All other filters were from Pall Corporation (Cornwall, UK). Buffers, salts, and cosolvents were obtained from Sigma-Aldrich (St. Louis, MO), EM Science (Gibbstown, NJ), EMD (Gibbstown, NJ), and Acros (NJ). Reagents for negative stain electron microscopy were purchased from Electron Microscopy Sciences (Hatfield, PA). Cytotoxicity assay reagents were from Invitrogen (Carlsbad, CA) and VWR (Westchester, PA), and the 3-(4,5-dimethylthiazol-2-yl)-5-(3-carboxymethoxyphenyl)-2-(4-sulfophenyl)-2H-tetrazolium, inner salt (MTS) solutions were from Promega (Madison, WI).

The identities of all synthetic peptides were confirmed by MALDI-TOF mass spectrometry at the Texas A&M University Protein Chemistry Laboratory. Purity was confirmed by an analytical 15 RPC column attached to an Akta FPLC/HPLC hybrid using a water/acetonitrile (with 0.1% trifluoroacetic acid) gradient. Data acquisition was facilitated by complimentary software associated with each instrument, and data analysis was performed using Kaleidagraph® software (Synergy software, Reading, PA).

Peptide synthesis

The procedure for solid-phase peptide synthesis and subsequent purification was modified from a previously described method.[94] The peptides were synthesized using standard Fmoc chemistry with N-methyl-2-pyrrolidinone (NMP) as the solvent. Wang resin was used, and both termini were left unblocked in the final peptides. A 'tea bag' method was used where the resin was contained in a sealed mesh bag for easy transference between containers. NMP, N,N-Diisopropylethylamine (DIPEA), 1-hydroxy-7-benaotriazole (HOBt), O-(1H-benzotriazole-1-yl)-N,N,N',N'-tetramethyluronium hexafluorophosphate (HBTU), and amino acids (Fmoc-Ala-OH, Fmoc-Asn(Trt)-OH, Fmoc-Gly-OH, Fmoc-Ile-OH, Fmoc-Leu-OH, Fmoc-Lys(Boc)-OH, Fmoc-Met-OH, and Fmoc-Ser(tBu)-OH) were used for each synthesis, and the scale was 0.1 mmol of resin (0.74 mmol/g) with five fold molar excess of HOBt, HBTU, and amino acids in 5 mL NMP.

Each round of solid-phase peptide synthesis consisted of three steps (Fig. 3). First, 20% piperidine in NMP was used for two periods of 3 minutes and 7 minutes to remove the protecting group on the resin or preceding residue and prepare it for the addition of an amino acid. Second, while the mesh bags filled with resin were washed 10 times with NMP to ensure removal of all piperidine, 5 mL of NMP was combined with HOBt, then with the amino acid/HBTU mixture and a 10 molar excess of DIPEA. Third, the amino acid solution was added to the 'tea bags' and the combination was covered with foil and was gently agitated for at least 4 hours and as long as overnight. After the allotted time,

the ‘tea bag’ was washed with NMP and the process repeated until the peptide was complete. Then the ‘tea bag’ was washed again with 20% piperidine and 5 times with NMP and 5 times with ethanol and allowed to dry overnight in a fumehood.

Step	20% piperidine	NMP	Amino acid/HOBt/HBTU/DIPEA
Purpose	Removal of α-amino protecting groups	Wash	Amino acid addition to peptide chain
Duration	3 minutes & 7 minutes	10 one minute cycles	4 hours - overnight

Figure 3. A schematic representation of the protocol for solid phase peptide synthesis used for all peptides.

After the peptides were synthesized, the ‘tea bags’ were submerged in 5 mL of Reagent R (4 mL trifluoroacetic acid, 0.5 mL thioanisone, 0.3 mL ethanedithiol, and 0.2 mL anisole) for two hours. Reagent R was used to cleave the peptide from the resin, remove the side-chain protecting groups of Fmoc-Asn(Trt)-OH, Fmoc-Lys(Boc)-OH, and Fmoc-Ser(tBu)-OH, and ‘scavenge’ the newly freed protecting groups to ensure that they did not react with the peptide. The resulting mixture was added to 30 mL of cold methyl-tert-butyl ether in a 50 mL Falcon tube and placed in a flammable storage freezer overnight to induce precipitation of the peptide. Then the Falcon tubes were centrifuged at 4°C using a Beckman model J-6B centrifuge to pellet the peptide precipitate at 1,500 rpm for 15 minutes. The ether was decanted and the pellet dried by evaporation under a

fume hood. The dried pellet was redissolved in 5% Acetonitrile, frozen, and lyophilized to a white powder.

The powder was dissolved into 88% formic acid, filtered with a Acrodisc syringe filter with 0.22 μm Supor membrane, and purified by an Akta FPLC/HPLC hybrid using a prep 15 RPC column and a water/acetonitrile (with 0.1% trifluoroacetic acid) gradient and lyophilized to a white powder. FPLC buffers were filtered with 0.22 μm GV Durapore membrane filters.

Preparation of peptide stock solution

The peptides were dissolved in 88% formic acid and stored at -80° C. Prior to the start of an aggregation assay, stocks were thawed and the formic acid was neutralized with 10 M sodium hydroxide and diluted to 0.5 mL, 1 mL, or 2 mL, depending on the assay, providing a sodium formate buffer of approximately 180 mM at pH 5.5, pH 4.8, or pH 3.0. Prepared in this manner, the peptide in solution at time zero was all monomeric as judged by an analytical 15 RPC FPLC column.

Disappearance of monomer assay

The primary method used to monitor aggregation is a disappearance of monomer assay (DMA) introduced by Wetzel and co-workers.[55; 95] In this method, peptide samples of approximately 45 μM were incubated in the sodium formate buffer with agitation at 37^{o}C. At regular intervals, the samples were removed from the incubator and

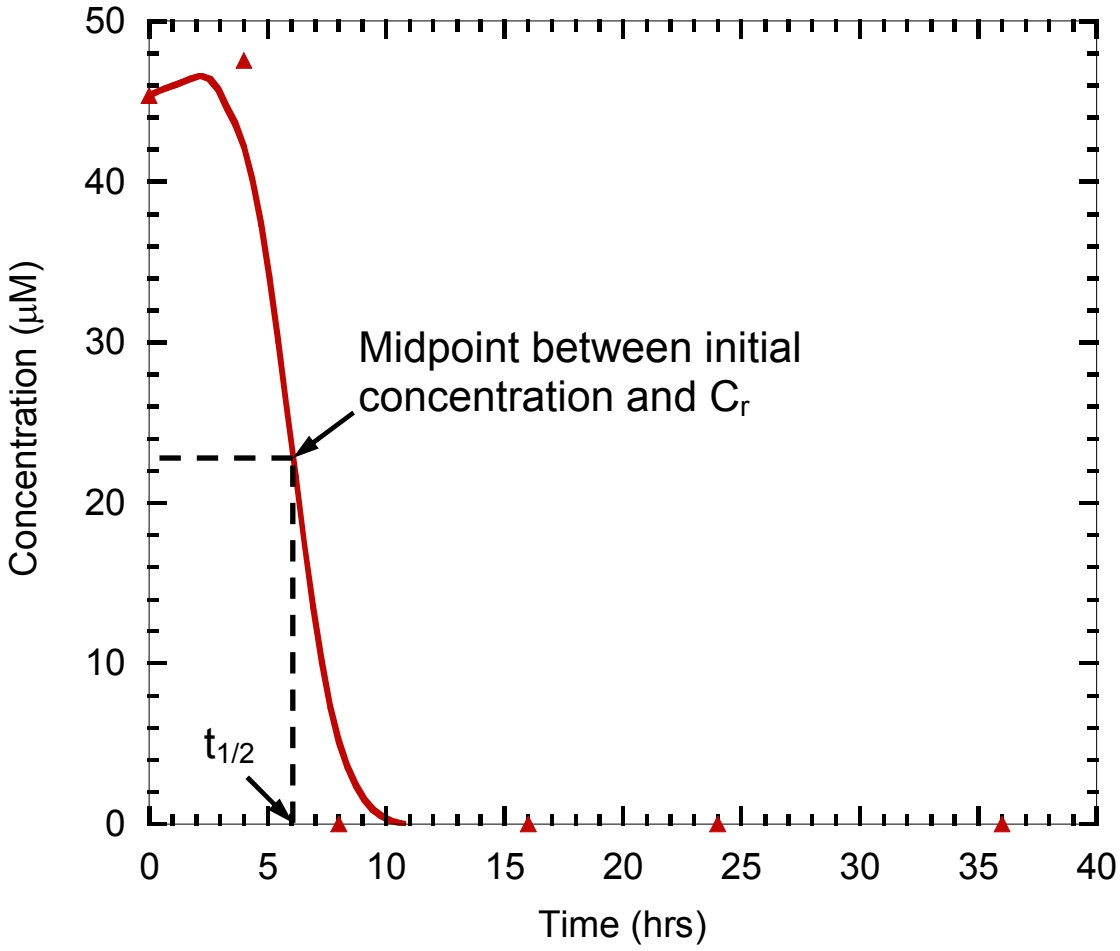

Figure 4. Sample data for Aβ(25-35) at pH 5.5 used to demonstrates how $t_{1/2}$ is measured. C_r is assumed to be 0 μM, and the $t_{1/2}$ is approximately 6 hours.

centrifuged with a table top centrifuge at 13,000 rpm for ten minutes. 50 μL aliquots were removed and injected onto an analytical 15RPC column with a water/acetonitrile (with 0.1% trifluoroacetic acid), which was connected to an Akta FPLC/HPLC hybrid and peak heights in mAU were recorded for analysis. Critical concentration (C_r) and half-time ($t_{1/2}$) as described in Chapter I were the parameters used to compare fibril formation. C_r was determined as the y-intercept once aggregation reached what appeared to be an equilibrium, and $t_{1/2}$ was measured as the midpoint between initial concentration and C_r (Fig. 4).

The quantitation of the peptide was facilitated by the use of a standard curve (Fig. 5) which was constructed using a desalted peptide in water with the concentration determined by a UV-Vis spectrophotometer at 220 nm. Due to the large signal of formic acid at 220 nm, desalting was required in order to obtain an accurate absorbance measurement. The stock peptide for the standard curve determination was desalted using a Harvard Apparatus Micro SpinColumn with G-10 gel, following the instructions enclosed.

Dynamic light scattering

Samples were prepared the same as for the DMA. Specifically, samples of approximately 45 μM were incubated in the sodium formate buffer with agitation at 37^{o}C. At regular intervals, samples were carefully transferred from a full 2 mL incubation tube to a cuvette using wide bore pipette tips to ensure that there was minimal

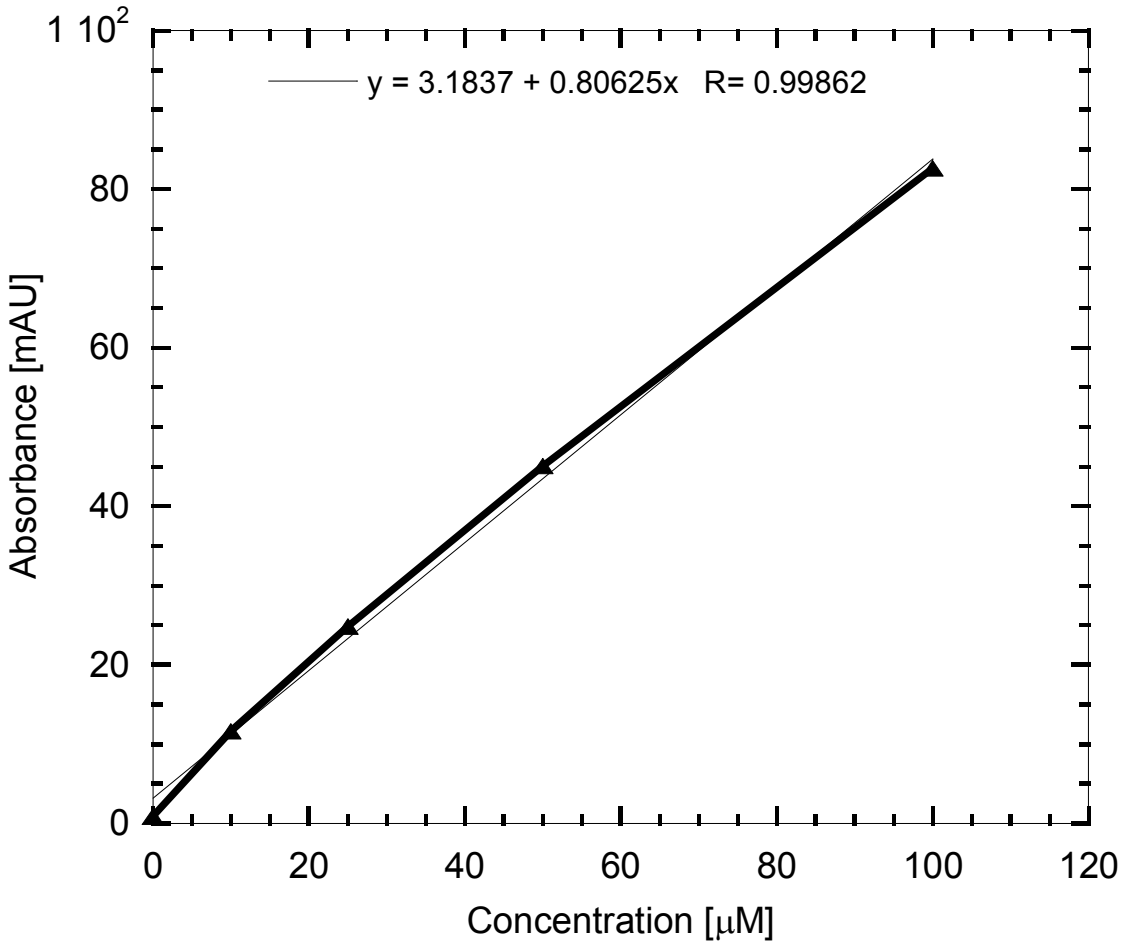

Figure 5. Standard curve of desalted Aβ(25-35) as measured by FPLC. The assay was conducted as described in the text.

disturbance of aggregates. Light scattering was measured with a Brookhaven Instruments Corp. Zeta PALS at 660 nm at a 90° angle. The baselines were measured, and mean diameters and size distributions were calculated using Brookhaven Instruments Corp. Dynamic Light Scattering Software Ver. 3.55. Once the light scattering was measured, the samples were transferred back to a 2 mL incubation tube using wide bore pipette tips, and incubation was allowed to continue at 37^{o}C with agitation.

Thioflavin T fluorescence

Thioflavin T (ThT) fluorescence was used as one confirmation for amyloid formation. The protocol was modified from previous work.[50] 200 μL samples were prepared with 10 μM ThT, 15 μM peptide, and 50 mM sodium phosphate at pH 6.0 in a Costar clear bottom 96 well plate. The plate was sealed with Axygen Scientific aluminum sealing film and incubated at 37°C with gentle agitation over the course of 24 days. A Spectra Max Gemini was used to measure the fluorescence signal, and SOFTMax Pro 5.1.1 was the program used to control the instrument. The excitation wavelength was 440 nm and emission wavelength was 485 nm. The resulting fluorescence signals were divided by the blank sample with ThT and no peptide, and those are the values reported.

Electron microscopy

Samples identical to those for the DMA were prepared by applying 5 μl of sample onto freshly glow-discharged formvar-carbon coated 400-mesh copper gilder grids and left

for 1 minute to adhere. Grids were then stained for 15 seconds using a 2% (w/v) aqueous solution of uranyl acetate (pH 4.5) and then blotted dry. Specimens were observed on a JEOL 1200EX transmission electron microscope operating at 100 Kv. Images were recorded on Kodak 4489 film at calibrated magnifications and scanned to a computer.

Brain endothelial cell cytotoxicity

This method measures the mitochondrial activity of mouse brain endothelial cells, which can be translated into cell viability. Peptides were desalted using Harvard Apparatus Micro SpinColumn with G-10 gel, leaving the peptide in water at neutral-range pH. Mouse brain endothelial cells (C57Bl/6) were prepared by the Jane Welsh lab at the Texas A&M College of Veterinary Medicine according to previous work.[96] Frozen cells were received and thawed in 37°C water bath for approximately one minute. Cells were then transferred to a T75 flask coated in a 1 mg/mL gelatin mixture, and were incubated with 12 mL of media.

For each assay, cells were incubated with 2 mL of 0.25% trypisin-EDTA at 37°C for 3 minutes to remove the cells from a T75 cell culture flask. The reaction was stopped with the addition of 2 mL of Iscove's Modified Dulbecco's Medium (IMDM) complete media containing 10% fetal bovine serum (FBS), 1% antibiotic/antimycotic, and 1% L-glutamine. The cells were collected by centrifugation (2000 rpm) for 5 minutes. The media was aspirated off and replaced with 1 mL of fresh complete media. Re-suspension was accomplished with repeated gentle pipetting. Using a Bright-Line

hemocytometer, the cells were counted and plated in complete media in a cell culture treated 96-well plates at 7000 cells per well. Cells were incubated overnight at 37°C in 5% carbon dioxide (CO_2 incubator from Nuaire, Inc in Plymouth, MN).

Before treatment with peptide, the 96-well plates were rinsed with plain treatment media to remove serum. Cells were treated with varying concentrations of peptide and 1% serum in 100 µL. Cells treated with antibody and peptide received 50 µL of antibody first, then 50 µL of peptide and 1% serum for a final concentration of 10 mg/mL of antibody in a total volume of 100 µL. Antibody was allowed to incubate for 30 minutes before the peptide was added in 50 µL sample for a total of 100 µL. Cells were incubated for 24 hours at 37°C and 5% carbon dioxide.

To measure cell viability, 20 µL 3-(4,5-dimethylthiazol-2-yl)-5-(3-carboxymethoxyphenyl)-2-(4-sulfophenyl)-2H-tetrazolium, inner salt (MTS) solution was added to each well and allowed to incubate for 2 hours, then absorbance was measured at 490 nm. Active mitochondria convert the MTS to formazan, which indicates healthy cells; no conversion suggests a reduced number of active mitochondria and therefore, cell death. This is an indirect measurement of cell viability and does not signify apoptosis.

CHAPTER III

Aβ(25-35) AMYLOID FORMATION REVISITED: A MODEL WITH A TWIST

Introduction

Over 5 million people in the United States have the neurodegenerative disorder, Alzheimer's disease (AD).[2] AD and other similar diseases are termed amyloid diseases since the main hallmark is the presence of amyloid plaques in affected tissues. Within the plaques are fibrils, which are misfolded proteins or peptides arranged in β-sheet conformation. The peptide found in plaques from patients with AD is Aβ(1-42), which is a well characterized amyloid peptide that is a product of cleaving the amyloid precursor protein (APP).[39; 97] It is the aggregation of this peptide that is thought to be a cause of AD.

There have been several models proposed for the mechanism of amyloid formation; one of the most popular is called nucleated polymerization, where the initiation of fibril formation depends on a slow nucleation step.[98-100] The nucleated polymerization model has three distinct steps: nucleation, elongation, and equilibrium. Nucleation and the associated lag time is necessary to form a nucleus, which is an oligomer of appropriate size consisting of misfolded protein or peptide that is able to initiate amyloid formation.[98; 100] Elongation is the spontaneous formation of fibrils by addition of peptide to the nucleus. Equilibrium is the final stage where fibrils are the dominant species and the suspension is relatively stable. This basic model, or variations of it, appear to

describe the kinetic process of amyloid formation in polypeptides, but doesn't address some other important aspects of amyloid diseases.

For many years, it was assumed that the density of amyloid plaques directly reflected the progression of disease; however, in more recent years, it has become apparent that the correlation between plaque density and neurodegeneration is not as strong as expected.[21; 25; 101] With this in mind, other aspects of the aggregation process has been studied, and there appears to be a higher correlation between the concentration of soluble oligomers found in the early stages of amyloid formation and progression of AD.[21; 22] Consequently, it has been suggested that these early soluble oligomers are the toxic species in the amyloid formation process and are responsible for the disease.[23-26] Therefore, it is important to detect and characterize these intermediate steps of amyloid formation in hopes of further identifying the toxic species. Unfortunately, it is complicated to study these early oligomers because they are usually transient, difficult to isolate, and part of a heterogeneous population of species present at the early stages of amyloid formation.

In this study, we utilize an eleven residue fragment of Aβ(1-42), termed Aβ(25-35), that forms amyloid fibrils similar to the full length peptide and is cytotoxic like the full-length peptide.[18; 102-110] We examine the aggregation of Aβ(25-35) at pH 3.0, because at this low pH we are able to detect and characterize several intermediates in the aggregation process. To observe the process, we use an FPLC assay that measures the

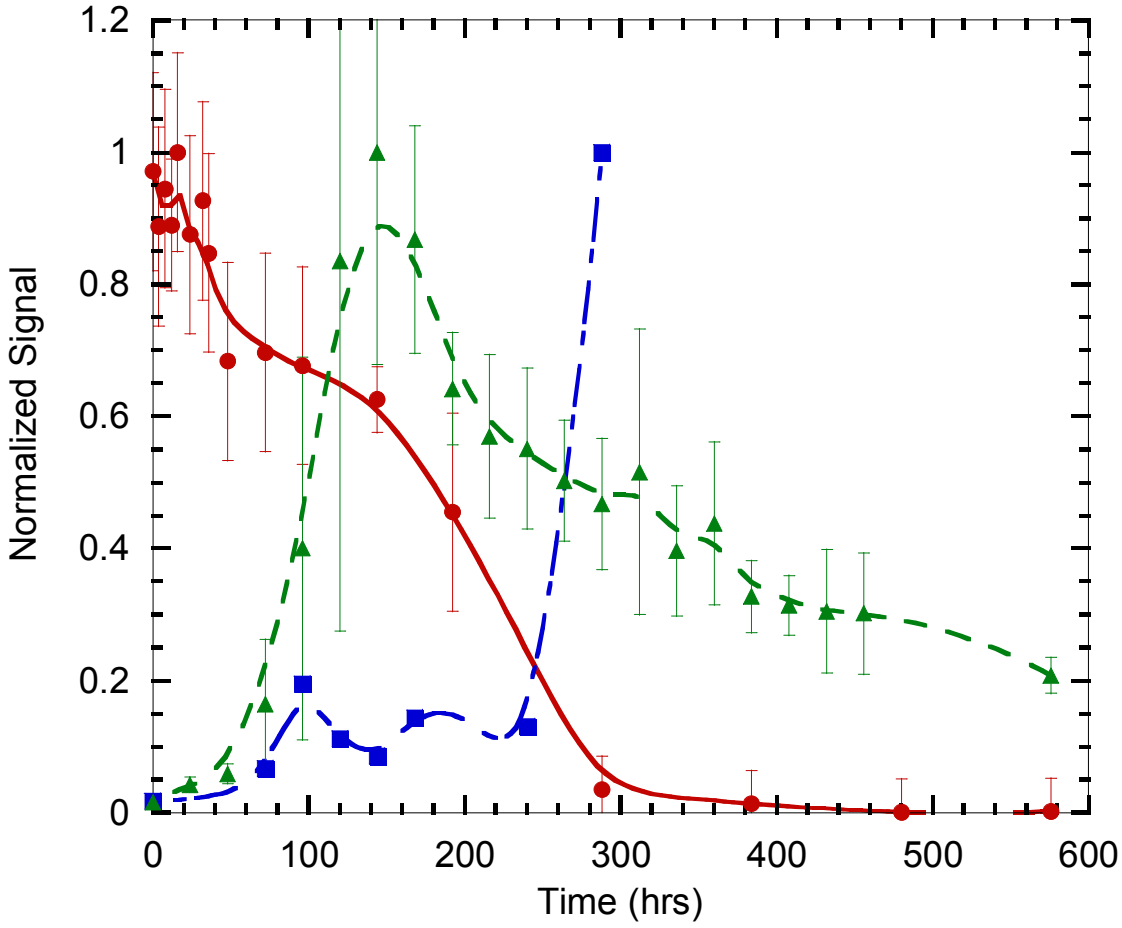

Figure 6. The time course for amyloid formation in Aβ(25-35) as monitored by several different probes. The disappearance of monomer assay (red circle), dynamic light scattering (blue square), and ThT fluorescence (green triangle) results are shown. The error bars denote standard deviation between experiments. The curves through the data points are meant to guide the eye.

disappearance of the monomeric peptide, as well as dynamic light scattering, electron microscopy, and Thioflavin T (ThT) fluorescence, a standard amyloid specific assay. With the combined strengths of these four methods, we are better able to follow the process of aggregation from monomeric peptides to macroscopic fibrils and gain some insight into the amyloidosis process.

Results

Disappearance of monomer

The starting point for our aggregation process is the monomeric peptide; therefore, it is the first logical species to monitor. To do this, we use a disappearance of monomer assay (DMA), which utilizes a chromatographic separation (FPLC) and quantitation method to measure the changes in monomer concentration over time. As shown in Figure 6, the concentration of the monomeric peptide fluctuates between 39 and 46 μM for the first 40 hours, while the expected initial concentration is 45 μM. Thereafter is a period of approximately 250 hours where the concentration decreases from 39 μM to 2 μM. Within this transition region, between 50 and 100 hours, there appears to be an intermediate step in the aggregation process. At the end of this period, and certainly around 290 hours after the start of the assay, the monomeric peptide concentration is essentially undetectable, and remains that way indefinitely.

Appearance of oligomeric intermediate species

To detect and characterize any intermediates, we utilize dynamic light scattering (DLS)

to measure the mean diameter of the aggregates in suspension. In a majority of samples, specifically those between 80 and 290 hours where the disappearance of monomer assay is in the transition region (Fig. 6), we see two very distinct populations by DLS: a minor population with particles of ≈180 nm in diameter, and one major population with particles of ≈ 4 μm in diameter (Fig. 7). There is also limited evidence of an extremely small population of much larger aggregates, on the scale of 10 μm. This significantly larger species only constitutes a few particles in the entire sample. Due to this varied population, we use the normalized mean diameter in Figure 6.

The first instance of a measurable oligomeric species is as early as 30 minutes after the assay begins, and this first oligomer has a mean diameter of approximately 400 nm (Fig. 6). The size of these intermediates increases over the first 80 hours. The intermediate mean diameter remains relatively constant, though it varies between 3 to almost 5 μm over the next 160 hours. The final stage of aggregation as measured by the DLS is roughly 290 hours into the reaction when the effective diameter of the dominant species jumps to > 20 μm.

Formation of amyloid

The amyloid specific assay that we employ is thioflavin T (ThT) fluorescence. ThT is a fluorescent dye that binds to amyloid fibrils, and possibly to prefibrillar species as well.[111-116] When bound to amyloid, ThT will fluoresce several orders of magnitude higher than unbound ThT, providing a sensitive test for presence of amyloid.[111-116]

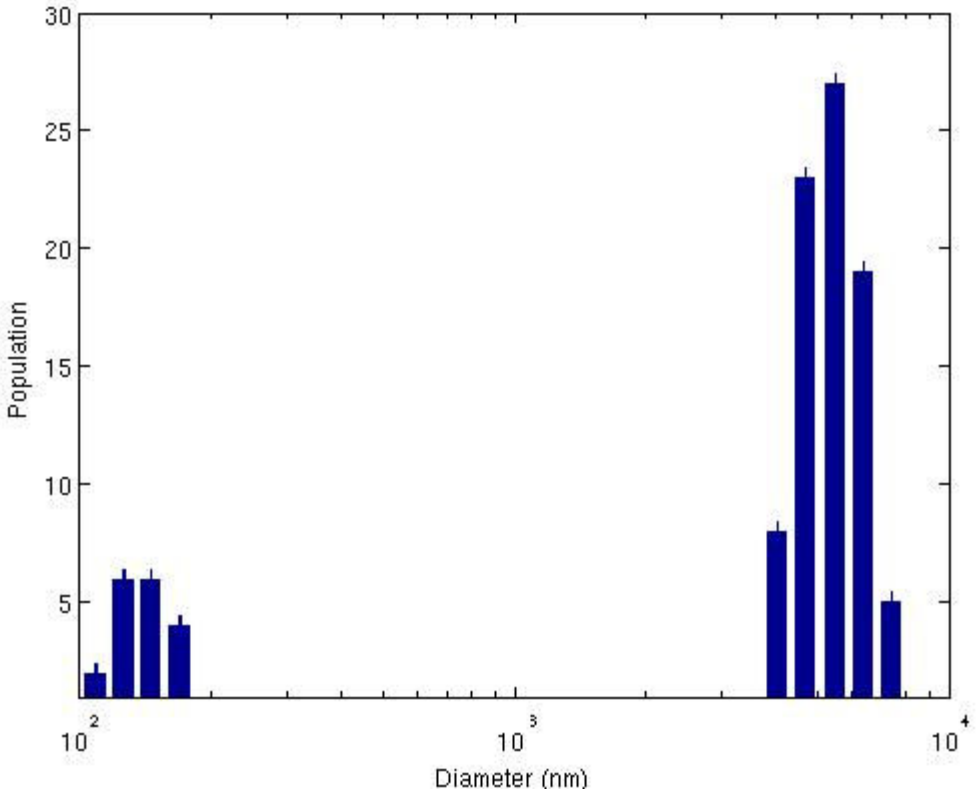

Figure 7. Size distribution of aggregates as measured by DLS at 120 hours.

For the first 50 hours, the fluorescence signal is small and constant (Fig. 6). However, as early as 70 hours, we see a sharp increase in the fluorescence signal that continues to rise over the next 70 hours, to reach a maximum signal 140 hours after the start of the assay. It is after this point that the signal begins to decrease on a much longer time scale than the initial increase in fluorescence. Then, at 380 hours, the decrease appears to perturb until the last time point at 580 hours, where the fluorescence signal is approximately 20% of the peak signal.

Electron microscopic characterization

Together, the methods described above allow us measure the disappearance of the monomeric peptide along with the appearance of intermediates and amyloid fibrils. The last method that we use, electron microscopy (EM), traverses most of the aggregation process from the initial small aggregates to the fibrils at the final stage of aggregation. With the micrographs taken over the course of the assay, we see snapshots of the aggregation process in order to better understand some features of the aggregation process that are not as readily observed using other methods. Despite the heterogeneity of the aggregates in the fibril formation process, we have attempted to show micrographs that represent the major species found at that point in time to provide the most accurate description of the aggregation process.

The first observable aggregates are found within the initial 24 hours. These aggregates are spherical and are as small as 5 nm and as large as 20 nm in diameter (Fig. 8a). At

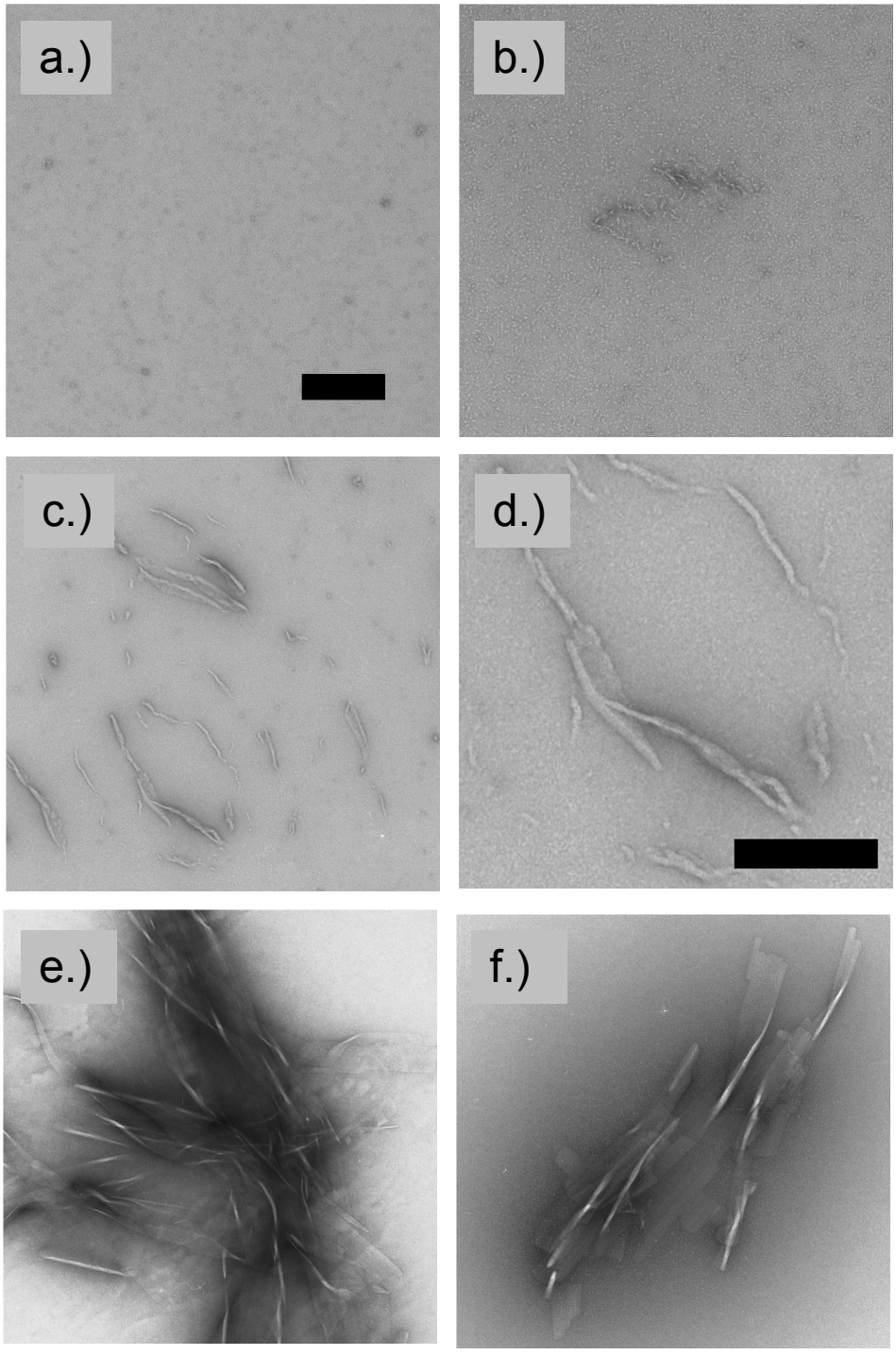

Figure 8. Negative stain electron micrographs of Aβ(25-35) recorded at various times during amyloidosis. (a.) 24 hours, (b.) 96 hours, (c.) 144 hours, (d.) rolled up sheet at 144 hours, (e.) 290 hours, and (f.) 480 hours. The scale bar in (a.) is 250 nm, and applies to all micrographs except (d.), where the scale bar is 100 nm.

around 100 hours, the 5 nm spherical aggregates are still present, though larger filamentous aggregates are also observed (Fig. 8b). The filaments shown here are approximately 100 nm in length and 5 nm wide, and upon closer examination, seem to be composed of the 5 nm spherical aggregates. However, there is evidence of longer filamentous aggregates beneath a thin sheet of peptide. We do not show the areas of the grid with the thin sheet of peptide, as it makes the filamentous aggregates difficult to distinguish. After 140 hours, there are a variety of aggregates observed (Fig. 8c). There are chains of the spherical aggregates that range between 50 and 550 nm in length, as well as a light dispersion of the small spherical aggregates. However, the largest population is a filamentous aggregate that appears to be rolled sheets of peptide and there are several instances of filaments in the middle of the process of rolling up into a tube. These fibrillar tubes, not including the peptide sheet as yet unrolled, are all approximately 10 nm in diameter and range in length from 60 nm to upwards of 380 nm (Fig. 8d). We continue to see these rolled sheets of peptides for the next 48 hours.

As early as 192 hours, there are fibrils present that are over 500 nm in length and approximately 20 nm wide (Fig. 8e). We also see that there are rigid plates of peptide that appear crystal-like, and in some cases, these plates appear to twist in a similar fashion to amyloid fibrils. These plates and twisted plates are all over 100 nm in width and have a large range of lengths, from 300 nm to over 1000 nm. After extensive aggregation, 480 hours, there are more of the rigid plates while a substantial presence of the twisted sheets remains (Fig. 8f). Our estimate is that essentially all of the total

peptide is incorporated into these plates and twisted sheets.

Discussion

In recent years, evidence has been amassed that shows amyloid plaque density cannot alone be used to determine the progression of disease in Alzheimer's patients.[21; 25; 101] Instead, more emphasis has been placed on studying the steps of amyloid formation since the early oligomers have been implicated in neurodegeneration and cell death.[21-26] Here, we show a modified version of a model (Fig. 9) that has recently been put forth and is growing in popularity.[117] This model suggests the fibril formation process can be divided into distinct stages. The monomeric peptide or protein reversibly aggregates into small oligomers, which in turn reversibly form larger aggregates. Once these larger aggregates appear, there is an uncharacterized transition into prefibrillar species, and it is assumed that at this stage the process becomes irreversible. The final step is then the formation of amyloid fibrils by another irreversible process. In order to gain a more complete understanding of the process of amyloid formation in a fragment of the Aβ peptide, we employ a number of biophysical methods in the current study. Each of these methods investigates a different step of the aggregation and therefore, collectively, a more complete picture of the step by step process of amyloid formation can be developed.

Before discussing the results in more detail, it should be pointed out that each of the methods utilized has some limitations. The DMA is limited in that it does not show

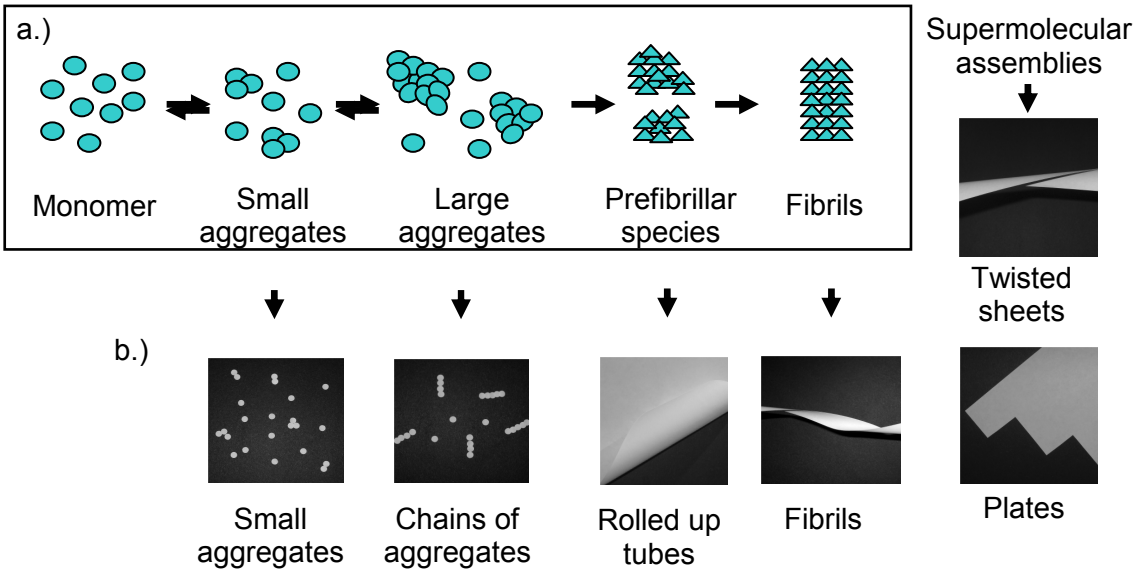

Figure 9. Comparing a general model of amyloid formation to electron microscopy data. (a.) A general model of amyloid formation as adapted from Ref 114. The circles indicate native or native-like structure of peptides or proteins and triangles indicate peptides or proteins that have undergone a structural change that commits them to amyloid formation. (b.) Models of the species observed by electron microscopy that explain the relationship between the electron micrographs in Fig. 8 and the general literature model. The picture of rolled up tubes is magnified to show detail.

how the monomeric peptide assembles, only that it disappears. Also, the DMA can partially disaggregate any loosely associated oligomers that may be in suspension, therefore, it is really reporting on the concentration of monomeric peptide and any weakly-associated aggregates. The DLS assay also has some limitations, especially for the characterization of samples that are heterogeneous with respect to size, shape, and distribution of aggregates and oligomers, like our amyloid samples. Characterization of a complex mixture is difficult, and parsing the bulk data into individual components requires some assumptions about the shape and size of each species. Nonetheless, DLS provides a characterization that is useful in our attempt to understand amyloid formation in this peptide system. While the ThT fluorescence assay is popular in the amyloid field, there are several potential limitations that must be heeded. First, as a fluorescent measurement, it is difficult to quantitate in an absolute sense and even comparisons between samples are difficult except in a relative sense. Second, it is difficult to adequately apply a solution based characterization to samples that are really suspensions. Third, it is not known for certain what species in the mixture is binding ThT and causing the fluorescent signal to change. Finally, in EM, the method is limited by what aggregates will bind to the carbon support film as well as which aggregates can be stained and visualized on the grid. Even with all these limitations, we feel that our use of these multiple techniques helps provide a more complete picture of amyloid formation.

The first stage of the model is the monomeric peptide (Fig. 8a), and since there is observable overlap of the monomeric peptide and small aggregates, it is useful to discuss the first and second stages of the model together. As shown in Figure 7 (red circles), the monomer concentration fluctuates at the beginning of the assay, possibly due to the formation of small, loosely associated aggregates. This lag period lasts about 50 hours, in which time we observed oligomers with diameters reaching from 20 (by EM; Fig. 8a) to 400 nm (by DLS; Fig. 6, blue squares) that correspond to the second stage of the model (Fig. 8a). These aggregates are also visualized in the first panel in Fig. 8b. Despite the presence of aggregates at this early stage, there is no ThT fluorescence signal (Fig. 6, green triangle), indicating no fibril or fibril-like aggregates, which is to be expected since monomer and small oligomers appear to make up the solution.

Larger aggregates are considered the third stage of the model. As this stage is difficult to distinguish from the prefibrillar species in the fourth stage, they are discussed together (Fig. 8a). After the initial lag period observed in the DMA (Fig 6, red circles), there is a transition region where the monomer concentration decreases over a 250 hour time span. It appears that this is due to larger aggregates that are more tightly associated, and therefore sediment during centrifugation before injection into the FPLC (Fig. 9b, panels 2 & 3). As the monomer concentration decreases during this 250 hour time period, the overall oligomer size measured by DLS increases to diameters between 3 and 5 μm (Fig. 6, blue squares). Because this coincides with the region of the DMA curve where the monomer concentration is decreasing, these oligomers appear to be the committed step

of aggregation (Fig. 9a, stage 4). It is also possible that these aggregates are the nuclei, or the immediate precursors of nuclei that will lead to fibrils. Until these aggregates are formed, it appears that the aggregation process is reversible since the smaller aggregates seen using DLS can still dissociate to monomeric peptide on the FPLC. However, after 70 hours, there is a sharp increase in fluorescence that does indicate the presence of fibrils and fibril-like aggregates (Fig. 9a, stages 4 and 5). The large error bars that we see on the ThT curve between 96 hours and 170 hours are easily explained. The signal reported here is an average of 4 separate samples, and as amyloid formation is a stochastic process, these large errors suggest that the 4 samples form fibrils and fibril-like aggregates at slightly different times. This is supported by the significantly smaller error bars on many of the other ThT curve data points.

According to the EM data, small chains of the initial spherical aggregates are formed after 100 hours of the aggregation process (Fig. 8b). Over the course of the DMA transition region, these chains of aggregates (Fig. 9b, panel 2) appear to form thin sheets of peptide through some unknown mechanism, and then begin to roll up to form tubes approximately 140 hours into the process (Fig. 8c). This rolling up of the peptide sheet (Fig. 9b, panel 3) continues over the next 48 hours and appears to be the main process of filament formation. To our knowledge, this is a novel pathway unobserved with other peptides or proteins. Since this is where we observe the largest ThT signal, it is interesting to speculate that these tubes might be the species that binds the fluorescent dye. This idea would explain why there is a decrease in the ThT fluorescence since

these tubes transition into fibrils at approximately the same time as the decrease in fluorescence which occurs immediately after the peak at 140 hours and continues through the rest of stage 4 and stage 5.

The final stage of the model is characterized by a primary population of amyloid fibrils (Fig. 9a). The period where the monomer is no longer detected by the DMA is most likely where amyloid fibrils are the dominant species, and the system seems to have reached a stable end or possibly an equilibrium point. At 290 hours, when the monomer is undetectable, the oligomer size as measured by DLS rapidly increases until it reaches a diameter of 23 μm. These 23 μm aggregates are most likely amyloid fibrils (Fig. 9a, stage 5), based on their large size.

For the most part, the data presented herein appear to support many of the current models of aggregation found in the literature (Fig. 9a). However, our EM evidence also reveals some unexpected features of amyloid formation: the rolled sheets that are assumed to represent the precursors of fibrils as well as two more species that are observed after amyloid formation (Fig. 9b, panels 5 & 6). With extended incubation, plates and twisted sheets are the only species that are observed by EM, implying that the fibrils transition into these larger aggregates (Fig. 7f). We speculate that the fibrils grow in width to become the twisted sheets, because we observe the twisted sheets alongside amyloid fibrils at the 290 hour time point. Then, as the process continues these twisted sheets become rigid and flatten to form the crystal-like plates. Upon even further

incubation, it is anticipated that the plates would be the only species in suspension. This is certainly another interesting step of the aggregation process as it is typically reported in literature that fibrils are the final product and not the plates described here (Fig. 9). This also introduces another possible explanation for the decrease of ThT fluorescence as the assay continues; it is possible that the ThT binds the amyloid fibrils, but as the fibrils transition into the plates, the ThT either does not bind as well or does not identify the plates as amyloid.

Together, all of these data indicate an aggregation process that can be broken up into steps easily visualized by EM: (1.) the monomer quickly aggregates into small, spherical aggregates up to 400 nm in size in solution, (2.) these small aggregates come together to form chains of aggregates of approximately 4000 nm in size in solution, and that bind to ThT after 100 hours, (3.) by some unknown mechanism, at around 140 hours into the process, the chains of spherical aggregates transform into small sheets of peptide that roll up into fibrillar tubes which appear to bind ThT to give the highest fluorescent signal of the assay, (4.) these fibrillar tubes grow in size by another unknown mechanism into amyloid fibrils over 20 μm in length at approximately 480 hours, and then (5.) the fibrils grow in width to become twisted sheets and rigid, crystal-like plates of varying sizes. Using the data from this study, we have a better understanding of the process of amyloid formation, which is important for early detection, prevention, and treatment of amyloid diseases, especially as it appears that it is the early aggregates that are responsible for disease and cell death.

CHAPTER IV

SEQUENCE RANDOMIZATION AND ALANINE SCANNING MUTAGENESIS REVEAL RESIDUES 30-35 AS A CRITICAL REGION FOR AMYLOID FORMATION IN THE Aβ PEPTIDE

Introduction

Amyloid fibrils result from an ordered aggregation of certain proteins or peptides and is associated with over twenty human ailments such as Alzheimer's disease, type II diabetes, and dialysis related amyloidosis.[118] The most prevalent amyloid disease is Alzheimer's disease, which afflicts 5.3 million people in the United States alone.[2] Amyloid fibrils found in Alzheimer's plaques are primarily composed of Aβ(1-42), a well characterized peptide that is a product of cleaving the amyloid precursor protein (APP).[39; 97] Within this peptide, Aβ(25-35), an eleven residue fragment, is frequently studied because it is capable of forming amyloid fibrils that are similar to the full length wild-type peptide and it is also cytotoxic to many mammalian cells, including neuronal cells.[18; 102-110]

An important strategy to help understand the features of amyloid formation is to determine the smallest region of a protein or peptide that is capable of forming fibrils. The amyloid core, or critical region, has been defined as the portion of a peptide in the interior of the fibril structure, and it might be the initiation point for fibril formation. Determining the core of an amyloidogenic peptide would be a significant discovery

since it would provide a viable target region for drug binding in order to prevent aggregation. Though many have tried to find the critical region of amyloid formation in Aβ(25-35) using various methods, it is still unclear.[18; 119; 120] Methods that have commonly been employed to find cores include deletions or mutations that alter many of the physiochemical properties of the peptide that could influence aggregation, such as hydrophobicity, solubility, charge, and secondary structure propensity, any of which could be the actual cause of any changes in amyloid formation.

A previous study identified residues 33-35 as a critical region of the Aβ peptide by using successive terminal deletions.[18] Later, hydrogen/deuterium (H/D) exchange and NMR were utilized to determine the core as residues 28-35.[119] A series of scanning mutagenesis studies reported the minimum regions necessary for amyloid formation as residues 31-34,[29] residues 31-36,[30] and residues 32-33.[31] Each of these studies gave slightly different results, possibly because, with the exception of the H/D exchange studies, they changed the overall properties of the peptide – properties that have been shown to have an effect on amyloid formation and the prediction thereof.[29-31; 33; 41; 45; 51; 52; 54; 59; 121] The only exception being the H/D exchange studies that did not alter any of the physiochemical properties; however, this method searches simply for the protected portions of the peptide within the fibril structure, which might be larger than the core.

Here we use partial sequence randomization to minimize the changes in the overall physiochemical properties of the peptide to determine the critical region of Aβ(25-35) is

Aβ(30-35) (Table 2). Aβ(30-35) was able to aggregate similarly to Aβ(25-35), which in turn, aggregated like the full length Aβ(1-42), and disruption of this region inhibited amyloid formation. To further elucidate precisely which residues were critical, Ala scanning mutants of the peptide were also studied by a variety of methods.

Table 2. Sequence and amyloid formation of randomized peptides

Peptide	Sequence[a]	Aggregation[b]
Aβ(25-35)	GSNKGAIIGLM	+
NScr	**NGS**KGAIIGLM	+
'NScr	**GKSGN**AIIGLM	+
CScr	GSNKGAII**LMG**	--
'CScr	GSNKGA**LIGMI**	--
N/CScr	**NGS**KGAII**LMG**	--
MScr	GSN**IAIKG**GLM	--
II-MScr	GSN**IIAKG**GLM	--
IG-MScr	GSN**IGIKA**GLM	--

[a] Randomized regions are bolded

[b] (+) denotes aggregation; '(--) denotes no aggregation

Results

The primary method we used to study amyloid formation is a disappearance of monomer assay (DMA). Dynamic light scattering (DLS) was used to detect the presence and approximate size of aggregates. Thioflavin T (ThT) fluorescence, an amyloid specific fluorescent dye,[111-116] to confirm the presence of fibrils since the disappearance of monomer assay and DLS cannot distinguish between amyloid and other aggregates. Our final *in vitro* method was electron microscopy (EM) for visual confirmation of fibrils and other aggregates. These methods have been discussed in further detail previously

(Chapter III). To give a complete picture in this study, we also utilize an *in vivo* cytoxicity assay to determine the cytotoxic effect of Aβ(25-35), Aβ(30-35), and Ala mutant peptides on rat brain endothelial cells.

Partially randomized sequence peptides

Our first approach to elucidate the amyloid core of Aβ(25-35) involved partially randomizing the sequence of the peptide in order to maintain the overall physiochemical properties of the peptide while disrupting the core, and performing only the DMA along with ThT fluorescence. The peptides used in this study are shown in Table 1 and the randomized, or scrambled, sections are bolded.

Of the eight partially randomized peptides, only the two N-terminal scrambled peptides, NScr and ‘NScr, showed amyloid formation similar to wild-type Aβ(25-35). Both C-terminal randomized peptides, CScr and ‘CScr, were unable to form amyloid for up to one month of incubation. The N/CScr peptide, with both termini randomized, was also unable to form fibrils for up to one month. Interestingly, CScr and N/CScr both aggregated immediately as amorphous precipitates, not amyloid fibrils. The final set of peptides, are the MScr series: MScr, II-MScr, and IG-MScr. The II-MScr and IG-MScr, were synthesized to test the significance of two consecutive Glys versus two consecutive Iles on amyloid formation. MScr, II-MScr, and IG-MScr all showed no aggregation for up to one month. These results, in addition to what was observed previously,[18; 29-31] led

us to focus our study on the C-terminal region of Aβ(25-35), specifically the last six residues: AIIGLM.

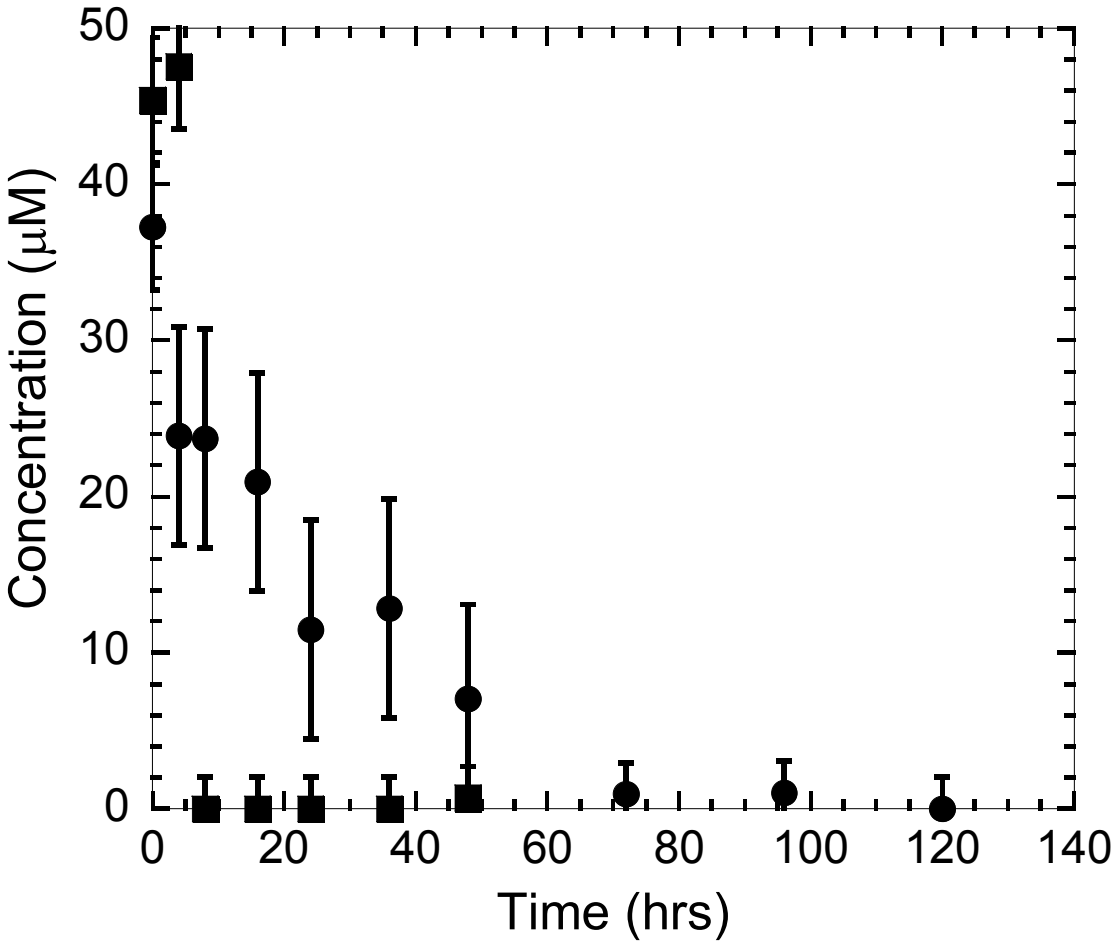

Figure 10. Disappearance of monomer assay of wild-type Aβ(25-35) compared to Aβ(30-35). Aβ(30-35) (circle) and Aβ(25-35) (square) in sodium formate buffer at pH 5.5 after agitating at 37° C. The graph shows the concentration of monomer as a function of time. Error bars are one standard deviation from the average value of four repeats.

Comparing the aggregation of Aβ(25-35) to Aβ(30-35)

The first step in establishing whether Aβ(30-35) was the critical region of amyloid formation was demonstrating that it could form fibrils like Aβ(25-35). As seen in Figure 10, the two peptides aggregated to the same extent; although, Aβ(30-35) took several days to aggregate as completely as Aβ(25-35), where the monomeric peptide was essentially undetectable after the first 8 hours.

Confirmation was needed that the peptides formed amyloid fibrils, therefore, we performed the disappearance of monomer assay concurrently with a ThT fluorescence assay for Aβ(30-35) and Aβ(25-35) (Fig. 11). For Aβ(30-35) the monomer concentration decreased within the first 10 hours, but we observed no increase in fluorescence until 50 hours, with no significant fluorescence until 100 hours. Note the difference in the shape of the ThT fluorescence curve as compared to Aβ(25-35) in Fig. 11b, where the fluorescence increased immediately as the monomer decreased, both occurring within 12 hours.

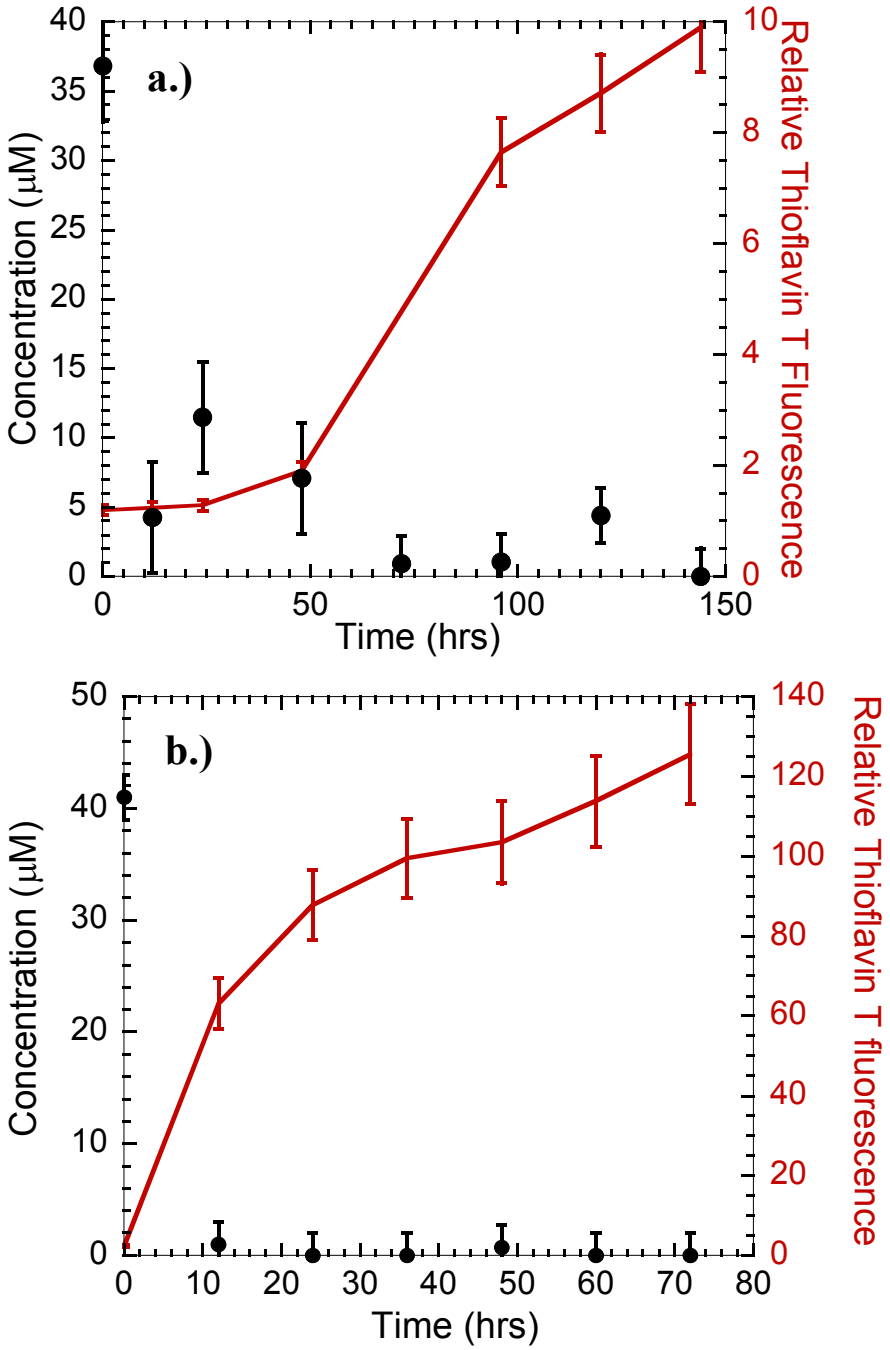

Figure 11. Disappearance of monomer assay data of Aβ(30-35) and Aβ(25-35) plotted against Thioflavin T fluorescence. (a.) Comparison of disappearance of monomer assay data (circle) to Thioflavin T fluorescence data (solid line) of Aβ(30-35). (b.) Comparison of disappearance of monomer assay data (circle) to Thioflavin T fluorescence data (solid line) of Aβ(25-35). The lines are used to guide the eye. Error bars are one standard deviation from the average value of four repeats.

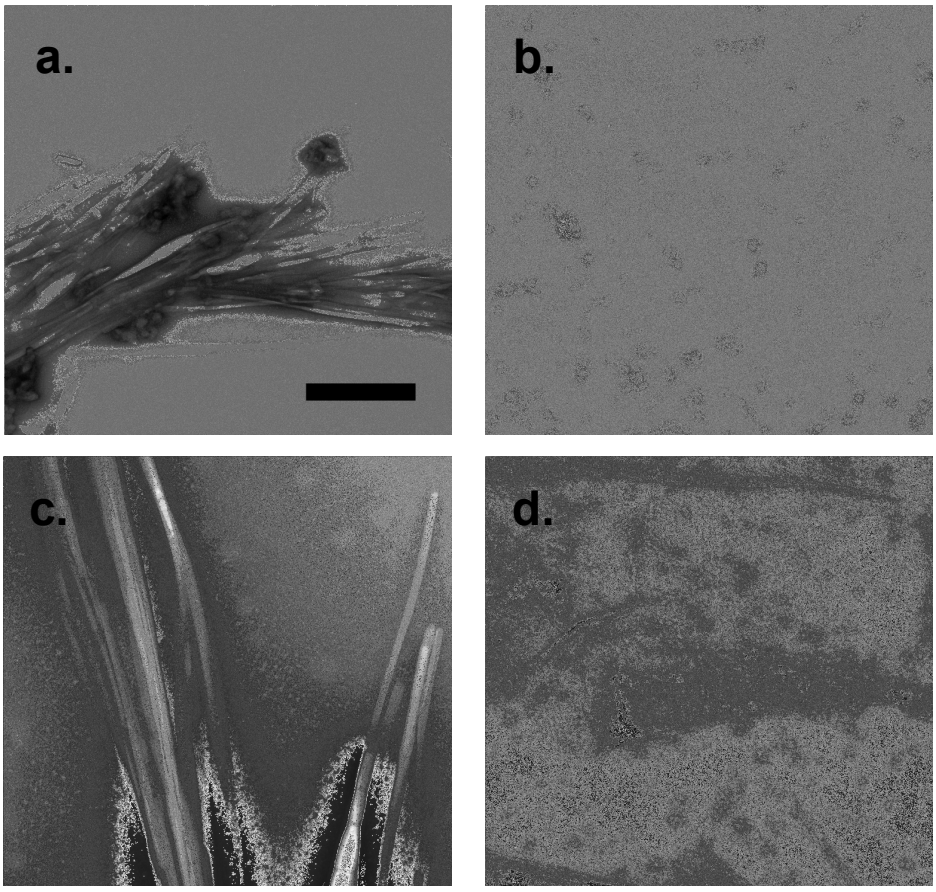

Figure 12. Negative stain electron micrographs of Aβ(30-35) and mutants. (a.) Aβ(30-35) fibrils and plates present after 144 hours, (b.) Aβ(30-35) spherical aggregates present after 48 hours, (c.) G33A fibrils and plates, and (d.) I32A with thin sheet of protein overlaying spherical aggregates. Scale bar is 300 nm.

As a visual confirmation of fibril formation, samples were analyzed by EM. Aβ(30-35) samples aged 50 hours gave spherical aggregates of varying sizes, averaging approximately 40 nm in diameter (Fig. 12b), however, these did not bind to ThT (Fig. 13). After the samples were aged 150 hours, ThT fluorescence was observed (Fig. 13) and fibrils were found along with crystal-like aggregates (Fig. 12a).

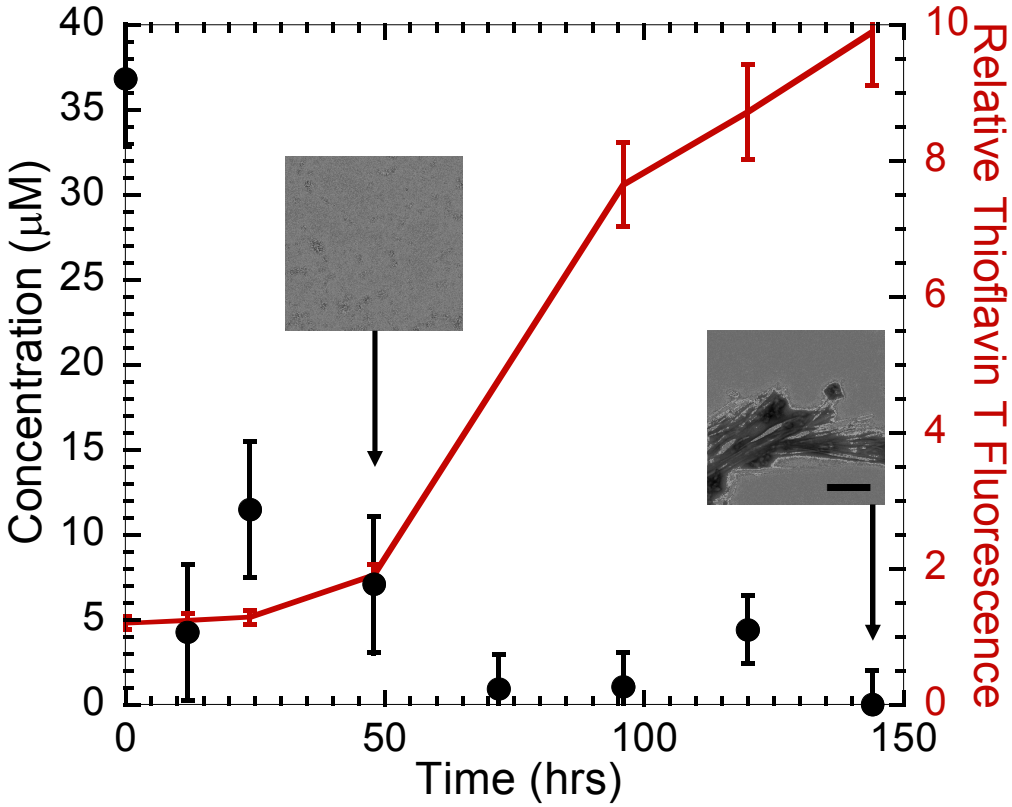

Figure 13. Correlation of disappearance of monomer assay data (circle) and Thioflavin T fluorescence data (solid line) to negative stain electron micrographs of Aβ(30-35). Placement of micrographs indicates time point when sample was taken and examined using electron microscopy: 48 hrs and 144 hrs. The lines are used to guide the eye. Error bars are one standard deviation from the average value. Scale bar is 300 nm.

Aggregation of Alanine scanning mutants

After confirming that Aβ(30-35) could form amyloid fibrils comparable to Aβ(25-35), we compared amyloid formation in Aβ(30-35) to the Ala scanning mutants. All of the Ala variants except G33A were unable to form amyloid fibrils for up to one week. This is significantly longer than the time scale of aggregation for wild-type Aβ(30-35), which showed substantial aggregation within 25 hours and full aggregation within 70 hours (Fig. 14). It is important to note here that G33A actually formed too quickly for our assay to measure at pH 5.5, where the peptide charge is near neutral; therefore, it had to be studied at pH 3.0 where the peptide had a positive charge and amyloid formation is slower due to charge effects. G33A monomer reached an equilibrium with the fibrils after approximately 25 hours, which was faster than Aβ(25-35) at pH 3.0. However, the amount of monomeric peptide left in solution was around 12 μM, significantly higher than with Aβ(25-35), where the monomeric peptide was undetectable. Aβ(30-35) did not form amyloid after two weeks at this low pH, though there was some evidence that the small aggregates in Fig. 12b were formed (data not shown).

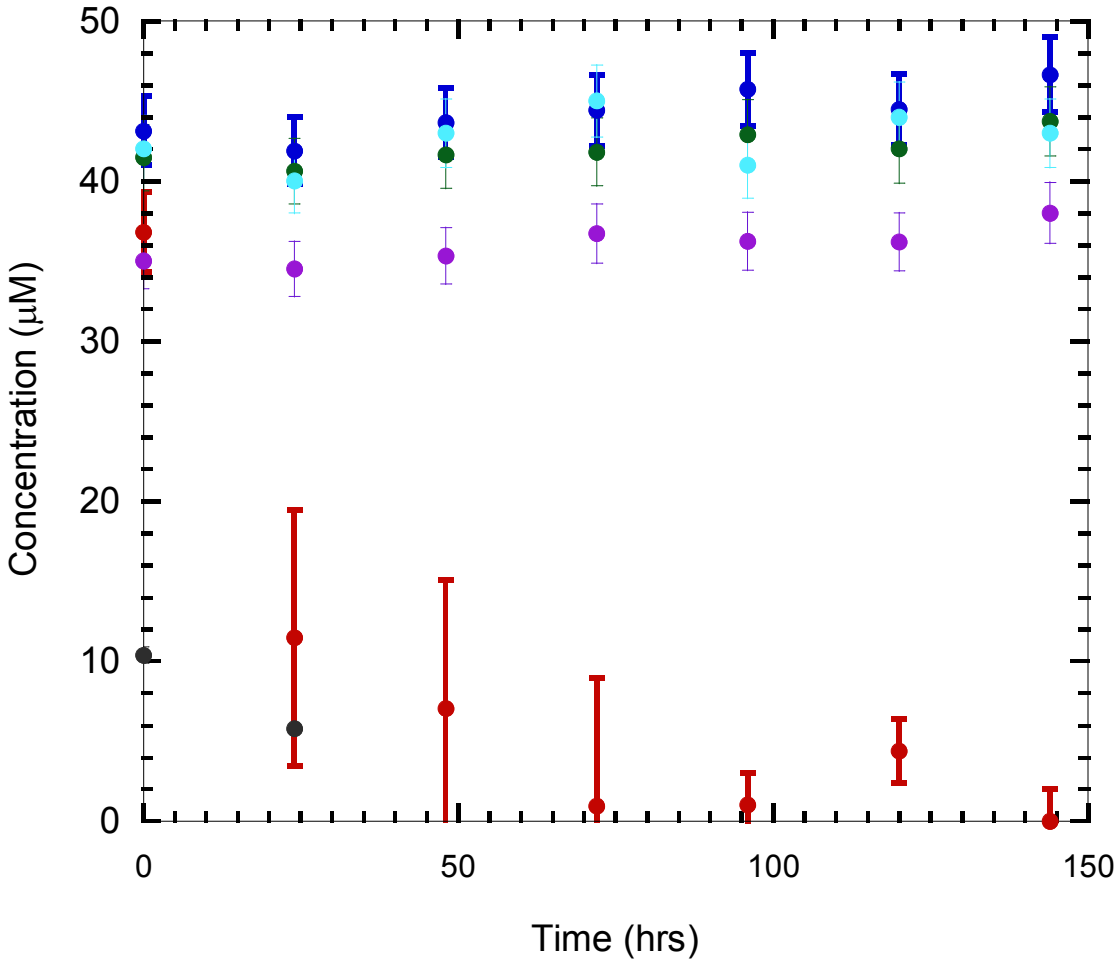

Figure 14. Disappearance of monomer assay data of Aβ(30-35) compared to Ala mutants at pH 5.5. Aβ(30-35) (red), I31A (blue), I32A (green), G33A (charcoal), L34A (purple), and M35A (cyan). Error bars are one standard deviation from average value of four repeats.

Dynamic Light Scattering

To better clarify and understand the aggregation and amyloid formation process, we employed DLS. With this method, we were able to measure the effective diameter, which is a weighted average, of the oligomers as well as observe the distribution of population sizes (Table 3). Interestingly, the DLS analysis of all the peptides showed

Table 3. Aggregate sizes of Aβ(30-35) peptides measured by dynamic light scattering

Peptide	Effective diameter[a,b]	Majority population size[a]	Minority population size[a]
Aβ(30-35)	1900	1080	uncharted
I31A	2600	60	900 & 7000[c]
I32A	900	1050	100 & 8400[c]
G33A	5100	uncharted	380
L34A	200	110	650
M35A	350	540	175

[a] Sizes measured in nm.
[b] Effective diameter is a weighted average of measure populations.
[c] Multiple minority populations were measured; the more populated species is listed first.
'Uncharted' indicates values that were larger than the measured range of the experiment.

aggregates of varying sizes after one week of incubation, despite appearing as monomer in the DMA (Table 4). However, Aβ(30-35), I31A, I32A, and G33A all had aggregates substantially larger than those found in the other variants. Aβ(30-35) aggregates had an effective diameter of about 1.9 μm, while I31A had aggregates with an approximate diameter of 2.6 μm (Table 3). I32A aggregates were 900 nm in diameter and G33A

Table 4. Sequence and aggregation of Aβ(30-35) peptides

Peptide	Sequence	DMA[a]	DLS[b]	EM[c]	ThT[d]	Cytotoxic[e]
Aβ(30-35)	AIIGLM	+	++	+	+	--
I31A	AAIGLM	--	++	--	--	+
I32A	AIAGLM	--	++	+ (spherical)	--	++
G33A	AIIALM	++	++	++	+	++
L34A	AIIGAM	--	+	--	--	++
M35A	AIIGLA	--	+	--	--	+

[a] Disappearance of monomer; (--) no aggregation; (+) aggregation; (++) extreme aggregation.

[b] Estimates aggregate size; (+) aggregates form; (++) aggregates > 900 nm diameter.

[c] Visible presence of aggregates; (--) no visible aggregates; (+) aggregates form; (++) extreme aggregation.

[d] Fluorescent confirmation of amyloid; (--) no amyloid (+) amyloid.

[e] Cytotoxicity towards rat brain endothelial cells at 10 μM; (--) no cell death; (+) limited cell death; (++) extreme cell death.

were approximately 5.1 μm. These large oligomer sizes were understandable for Aβ(30-35) and G33A as they both showed a rapid decrease in the monomer concentration, and tested positive for amyloid fibrils. What was surprising, though, was the presence of these large oligomers in the I31A and I32A samples as these two mutants did not appear to have a decrease in the monomer concentration, suggesting the absence of aggregation.

The other two mutants, L34A and M35A, of Aβ(30-35) showed aggregation by DLS also, though significantly smaller in size. The effective diameter of the L34A aggregates were approximately 200 nm, and M35A aggregates were approximately 350 nm in diameter (Table 3).

Fibril formation of Ala scanning mutants

As with wild-type Aβ(30-35), we tested the Ala scanning mutants for amyloid formation using ThT and EM. G33A was the only peptide to show ThT binding, though the signal was lower than that of Aβ(30-35). The electron micrographs of G33A had extremely large fibrils that appeared as twisted ribbons bundled together that were several thousand nanometers long and 50 nm in width (Fig. 12c). Only one other mutant showed aggregation with EM, however it was not amyloid; I32A had a very thin sheet of protein overlaying small, loosely associated spherical aggregates of approximately 40 nm in size that, when tested using FPLC, appeared as monomeric peptide (Fig. 12d and Fig. 14).

Cytotoxicity of Aβ peptides

We assessed the cytotoxicity of Aβ(25-35), Aβ(30-35) and all of the Ala mutants of Aβ(30-35) by an MTS assay that determines cell viability of rat brain endothelial cells by measuring the mitochondrial activity. Neither Aβ(25-35) or Aβ(30-35) were significantly cytotoxic at 10 μM, although at higher concentrations Aβ(25-35) was cytotoxic. In contrast, all of the variant peptides were cytotoxic to rat brain endothelial cells, even the peptides that demonstrated limited aggregation by other methods (Table 4). Of particular note are I32A and G33A, which were far more effective at killing cells than the other peptides, even at 10 μM, where Aβ(25-35) had little effect. This result was unexpected and rather puzzling.

Discussion

There are several methods that have been used in an attempt to determine the core amyloid regions of peptides and proteins: terminal deletions,[18] scanning mutagenesis,[29-31; 122] strategic proline mutations,[122] H/D exchange,[119; 123] proteolysis of fibrils,[124; 125] and very recently, solid state nuclear magnetic resonance in conjunction with DLS and ThT fluorescence.[126] To our knowledge, there have been no attempts to uncover the critical region of an amyloid-forming polypeptide using partial randomization of the sequence, as we have. The reason we chose to use partial randomization as our first step instead of using any of the other methods is tied into the pitfalls of several of the aforementioned methods: they search for the main region involved in fibril structure instead of the critical region that is most likely responsible for initiation of aggregation, or they change

the overall physiochemical properties of the peptide. It has been shown that changing hydrophobicity, secondary structure propensity, charge, and other physiochemical properties alters the ability of a peptide to form amyloid fibrils.[29-31; 33; 41; 45; 51; 52; 54; 59; 121] Therefore, with methods such as terminal deletions and scanning mutagenesis, the overall physiochemical properties of the peptide are altered, where partial randomization minimizes or avoids changes in the physical properties of the peptides.

To test this idea, we randomized different regions of Aβ(25-35). Our results indicate that the N-terminal region is not necessary for fibril formation since both NScr peptides were able to form amyloid like wild-type Aβ(25-35). Because both C-terminal (CScr) peptides as well as all three middle scramble (MScr) peptides were unable to form amyloid fibrils, we concluded that the core region for amyloid formation resides within the last six residues. Therefore, the C-terminal region was the focus for the rest of our study (Table 2).

It was important to show that the truncated peptide was capable of forming amyloid fibrils similar to the longer Aβ(25-35) since that would show that Aβ(30-35) contained the amyloid core necessary for initiation of amyloid formation. As shown in Figure 10, the truncated peptide aggregates to the same extent as Aβ(25-35), although Aβ(30-35) did require 70 hours to fully aggregate as compared to 8 hours necessary for all of the Aβ(25-35) monomer to disappear. This test alone did not show that Aβ(30-35) contains the amyloid core, though it did lend strong evidence that the core was present in the

hexapeptide. It also implied that if Aβ(30-35) did contain the core, the N-terminal portion of Aβ(25-35) was important for fibril formation, but not critical.

As a more definite test to determine whether Aβ(30-35) was able to form amyloid, we used both ThT fluorescence and EM for confirmation of amyloid fibrils (Figs. 11a and 12a). From these assays, we gathered that Aβ(30-35) formed fibrils and therefore, contained the amyloid core. However, these tests also revealed an important difference between Aβ(30-35) and the longer Aβ(25-35) that we had not been previously aware of: the presence of a measurable intermediate step in the aggregation of Aβ(30-35).

The initial DMA (Fig. 10) hints at the presence of the intermediate aggregation step for Aβ(30-35), although this intermediate was more clearly seen in the comparison between disappearance of monomer, appearance of ThT fluorescence, and the spherical aggregates observed using EM (Fig. 13). Between 10 and 50 hours, the monomer concentration of Aβ(30-35) had decreased, but fluctuated before reaching a lower equilibrium at 70 hours. Prior to 70 hours, there was a distinct lack of ThT fluorescence, suggesting that nothing amyloid or amyloid-like was present. Also at this stage of aggregation, we observed spherical aggregates with EM (Fig. 13). Similar spherical aggregates of various diameters have been reported previously in the longer Aβ(1-40) and Aβ(1-42) as well as other amyloidogenic proteins.[17; 127-134] In some cases, they were reported to be an intermediate step before fibrils were formed,[17; 128; 130-132; 134] as

appeared to be the case with Aβ(30-35); although in other peptides, these spherical aggregates appeared to be stable so that fibrils were not observed even after a longer incubation time.[129; 133]

This difference in the observable process of aggregation between Aβ(25-35) and Aβ(30-35) was further emphasized in Fig. 11, which showed the disappearance of Aβ(25-35) monomer in conjunction with the development of ThT fluorescence. Due to the immediate increase of Aβ(25-35) ThT fluorescence and our EM studies that was simultaneous with the disappearance of monomer, it appears that the monomer is forming amyloid fibrils directly with no measurable intermediate. Also of interest between the ThT fluorescence of Aβ(30-35) and Aβ(25-35) was the difference in the intensity of the fluorescent signal. Aβ(25-35) is known not to bind ThT very well due to the hydrophobic nature of the peptide and the charge on the ThT molecule. However, with Aβ(30-35) we removed the only charged residue from the peptide as well as the polar residues, leaving the hydrophobic core and the charged termini. Therefore, this truncated hydrophobic peptide should not bind ThT to near the same extent as the longer Aβ(25-35), which appeared to be the case.

The error values of each peptide were calculated in relation to the average value at each time point. Interestingly, the large error values of Aβ(30-35) as compared to the error values of Aβ(25-35) in Fig. 10 and the Ala scanning mutant peptides in Fig. 14, appeared to be a result of the transient nature of the spherical aggregates that could

associate or dissociate easily, giving a wide range of monomer concentrations. This was further supported by the smaller error values at time zero of Aβ(30-35) and during the equilibrium where most if not all of the monomeric peptide was aggregated (Fig 10 and Fig 14).

After demonstrating that Aβ(30-35) formed amyloid fibrils similarly to Aβ(25-35), we proceeded to scan the rest of the peptide with Ala mutations. Recalling the two parameters we use to compare amyloid-forming peptides, the critical concentration (C_r) that describes the extent of monomeric peptide conversion to fibril, and half-time ($t_{1/2}$) which relates to the speed of aggregation, the peptide that was most interesting in its result was G33A. This peptide was not only the one mutant that formed amyloid fibrils, but it actually formed fibrils better than wild-type, judging by the need of G33A to be studied at a lower pH than wild-type since lowering the pH inhibits aggregation of the peptides. G33A was certainly a faster amyloid former than Aβ(30-35) and Aβ(25-35), however with a higher final concentration than Aβ(25-35), G33A did not appear to aggregate to the same extent. The absence of aggregation of the other mutant peptides demonstrates that the other four residues, Ile31, Ile32, Leu34, and Met35, were critical for aggregation since mutating any of these four residues to Ala resulted in the loss of fibril formation. With G33A, the increase in amyloidosis did not mean that position 33 was not critical for amyloid formation. On the contrary, it showed that Gly33 is a rather important residue as mutating it to Ala notably increased the kinetics of fibril formation. Ala has higher β-strand propensity, hydrophobicity, and lower solubility as compared to

Gly. Due to these changes in the physiochemical properties, one would expect that there would be an increase in amyloid formation, which was exactly what we observed.

Substantial data in the literature have suggested that the oligomeric species is more likely to be the cause of cell death than the amyloid fibrils.[21-24; 26; 27] Therefore, of particular interest to us were the combined data from DLS and the cytotoxicity studies, though the results were certainly unexpected. In an aqueous environment, it is natural for hydrophobic peptides to aggregate, but the sizes of aggregates that we observed for I31A and I32A appeared to be extremely large (Table 3), considering that they dissociate easily enough to appear as monomer with FPLC (Fig. 14), and for only minor aggregates to be observed for I32A with EM (Fig. 12d). At first glance, it might appear that the presence of these large aggregates found in wild-type Aβ(30-35), I31A, I32A, and G33A were the cause of the cytotoxicity as I32A and G33A were profoundly toxic while L34A and M35A did not appear to have large oligomers and were not nearly as toxic (Table 4). However, I31A was found to have these large aggregates, but was decidedly less toxic than I32A and G33A. Also, wild-type Aβ(30-35) had these large aggregates, but was not found to be cytotoxic at 10 μM, which was consistent with the lack of significant toxicity of Aβ(25-35) at 10 μM found in this study as well as previous studies.[106; 135; 136] This implies that these large aggregates were necessary to cytotoxicity but not sufficient, which unfortunately leaves the key to what makes these peptides cytotoxic still very much in question. However, it did show that the ability to form amyloid fibrils is not a determining factor in cytotoxicity, further emphasizing the common hypothesis that cell

death is more likely caused by some oligomeric intermediate in the aggregation process rather than the final fibril product.[23-26]

To compare the experimental data to prediction, we utilized two programs that can be useful in determining the identity of the minimal region necessary for amyloid formation: TANGO[59; 91] from the Serrano laboratory and Waltz from the Switch laboratory.[92; 93] Both of these programs are easy to use and attempt to predict aggregation by examining physical properties of the peptide and the peptide environment. Waltz also considers structural parameters, though which parameters the program examines is not described.[92] To predict the portions of the peptide most likely to β-aggregate, both programs require the peptide sequence and specifics of the solution condition such as pH, temperature, or salt concentration. TANGO makes no claim to predict amyloid formation, only β-aggregation, which is not necessarily fibrillar; however Waltz is supposed to predict amyloidogenic sequences, which we expect to be the amyloid cores.

Both TANGO and Waltz were used to predict: (a.) if Aβ(25-35) and Aβ(30-35) would aggregate, and (b.) which residues were more likely to be included in the amyloid core. Waltz did not predict Aβ(25-35) or any of the peptides in this study to aggregate at all, which contradicted the aggregation documented in this study and in previous works.[18; 119; 120] Previously, Waltz had been shown to give accurate predictions in hsp10;[137] though perhaps not the entire core region, certainly part of the amyloidogenic regions

were correctly predicted. However, that was not the case with this collection of peptides as Waltz was unable to predict any region of fibril formation for the entire peptide.

TANGO, on the other hand, predicted that the C-terminal portion of Aβ(25-35), specifically residues 30-34 would be likely to β-aggregate. When the truncated Aβ(30-35) was used, TANGO still predicted aggregation, though not to the same extent as Aβ(25-35). We also analyzed the Ala scanning mutants for analysis and none of the mutants were predicted to have considerable aggregation other than G33A, which had a higher probability of aggregating than wild-type Aβ(25-35). M35A was also predicted to aggregate, however the probability was much smaller than the probability of the wild-type Aβ(30-35). This did not completely agree with our findings as G33A indeed formed amyloid better than Aβ(30-35), but M35A was unable to form fibrils. It appeared that for this peptide, TANGO, which only attempted to predict areas of β-aggregation, predicted the amyloidogenic segment in the C-terminal portion of Aβ(25-35) as found here. Also, TANGO did exceptionally well in predicting the amyloid formation of all the peptides, showing that simply as a predictor for β-aggregation, it performed better than Waltz.

To summarize, we found the amyloid core of Aβ(25-35) to be residues 30-35, and Ala scanning mutants were further used to confirm that every residue in Aβ(30-35) was important. Various tests showed that Aβ(30-35) amyloid formation had an additional

intermediate step that was not observed in Aβ(25-35) at pH 5.5. We also found that all of the Ala scanning mutants of Aβ(30-35) were still able to aggregate to varying extents as measured by DLS and were all found to be cytotoxic. This was a major difference from wild-type Aβ(30-35), which was capable of forming amyloid fibrils, but was not found to be cytotoxic. This demonstrated a significant divorce in the ability to form amyloid and toxicity, further supporting the popular hypothesis that the intermediate oligomers are responsible for cell death.[23-26] Combined, this information should help with the understanding of Aβ(25-35) and possibly even full length Aβ aggregation as it pinpointed the amyloid core of the peptide. With the amyloid core of Aβ(25-35) found, a critical region is now known that can be used as a target for preventing aggregation.

CHAPTER V

SOLUBILITY, HYDROPHOBICITY, AND β-STRAND PROPENSITY HAVE THE LARGEST EFFECT ON AMYLOID FORMATION OF Aβ(25-35)

Introduction

Currently, there are over twenty known amyloid diseases found in humans[118]. Due to this large number, there is much interest to identify what causes amyloid fibril formation. There is no obvious common physical characteristic among the various proteins and peptides that form fibrils; the amino acid sequence of amyloidogenic peptides and proteins varies from predominantly hydrophobic residues as in Aβ(1-42), primarily hydrophilic residues as in Sup35, or anything in between. Because of the sequence variety of amyloid forming peptides, it is necessary to discover which physiochemical properties contribute most notably to this ordered aggregation. It has recently been suggested that aggregation might simply be inherent to the peptide backbone as proteins with wide ranges of amino acid sequences can be induced to form amyloid.[45; 138-140] However, this does not explain why a single mutation to an amyloid forming peptide can have a significant effect on fibril formation. If ordered aggregation is solely caused by the peptide backbone, the side chains should not make a difference, and this has been shown to be untrue. This inconsistency has been acknowledged in part by the suggestion that perturbations of the backbone are responsible, rather than differences in the side chain interactions.[45] However, that still does not fully explain the notable differences in aggregation observed between peptides.

In recent years, research groups have created algorithms that use various factors to predict which peptide sequences will most likely form amyloid fibrils. TANGO is a program that considers hydrophobicity, β-sheet propensity, electrostatics, hydrogen bonding, and α-helix/β-turn competition when determining if a peptide will aggregate in a β-strand form.[59] TANGO does not claim to predict amyloid formation, yet it can be used as to screen large sequences for amyloidogenic regions. Dobson and co-workers have put forth several equations that attempt to predict aggregation rates and aggregation prone regions of peptides.[45; 48; 54] Their first prediction equation only considered change in hydrophobicity, change in charge, and changes in the free energy of folding from random coil to α-helix or β-strand to predict the aggregation rate of a mutant as compared to wild-type.[45; 48] In later papers, Dobson and co-workers also began to look at patterning of the residues, as well as extrinsic factors such as pH, peptide concentration, and ionic strength.[48; 54] Caflisch and co-workers also reported methods to predict aggregation rates and aggregation prone regions.[52] Their equation accounted for numerous additional properties, including solubility, solvent accessible surface area, parallel β-sheet, anti-parallel β-sheet, aromaticity, temperature, and several others.[52]

These methods are useful, though not ideal, because it is difficult, perhaps even impossible, to cleanly separate all the factors. If systematic studies could be performed that would quantitatively and individually measure how physiochemical properties – β-strand propensity, hydrophobicity, solubility, and residue charge – affect amyloid formation, the prediction algorithms could be revised to make more accurate predictions.

The values of the four physiochemical properties – β-strand propensity,[141] hydrophobicity,[89] solubility,[58] and residue charge – that we used for comparison between the twenty peptides in this study are shown in Table 5. The four factors listed above have been chosen because they all have been previously shown to have an effect on amyloid formation.[33; 40; 45-48; 51; 52; 54] Increased hydrophobicity and increased β-strand propensity are two properties that appear to encourage amyloid formation.[33; 34; 39-41; 46; 49] Increased charge, on the other hand, has been shown to decrease amyloid formation in most cases.[33; 44; 49; 53] However, in one study, the use of a Lys and Glu pairs actually promoted amyloid formation due to an electrostatic attraction that stabilized oligomers.[41] As for solubility, it was previously observed that RNase Sa and several variants are more likely to form amyloid fibrils at pH values at or near the pI, where these proteins are least soluble and have the smallest net charge yet the highest total number of charged residues, and as the pH of the solution moves further away from the pI, aggregation decreases.[50]

Table 5. Physiochemical properties of substituted amino acids to Leu34 in Aβ(25-35)

Amino acid	Hydrophobicity[a]	β propensity[b]	Solubility[c]	Charge[d]
Leu*	1.82	0.32	0.35	0
Ala	0.39	0.47	1.00	0
Arg	-3.95	0.35	1.59	+1
Asp	-3.81	0.72	1.63	-1
Asn	-1.91	0.40	0.80	0
Cys	0.25	0.25	0.45	0
Gln	-1.3	0.34	0.76	0
Glu	-2.91	0.35	1.58	-1
Gly	0.00	0.60	1.01	0
His	-0.64	0.37	0.90	0
Ile	1.82	0.10	0.31	0
Lys	-2.77	0.35	1.17	+1
Met	0.96	0.26	0.43	0
Phe	2.27	0.13	0.17	0
Pro	0.99	n.d.	0.55	0
Ser	-1.24	0.30	1.45	0
Thr	-1	0.06	0.76	0
Trp	2.13	0.24	0.13	0
Tyr	1.47	0.11	0.21	0
Val	1.30	0.13	0.39	0

[a] Modified from Ref. 89 Range: -3.95 (low hydrophobicty) to 2.27
[b] Values from Ref. 139 Range: 0.06 (high propensity) to 0.72 (low propensity)
[c] Normalized from Ref. 58 Range: 0.13 (low solubility) to 1.59
[d] at pH 7
* wild-type

The peptide we utilize here is Aβ(25-35), an eleven residue segment of Aβ(1-42), the primary component of the protein plaques associated with Alzheimer's disease.[39; 97] Aβ(25-35) is often used for amyloid studies due to its small size, ability to form amyloid fibrils similar to the full length Aβ(1-42), and cytotoxicity.[18; 102-110] In this study, mutations were made at the Leu34 position of Aβ(25-35), as this residue has been implicated as part of the critical region necessary for amyloid formation in several studies.[18; 29; 30] All of the mutants fell into one of three classes: Class I, which is similar to wild-type amyloid formation, Class II, which demonstrates significantly decreased

aggregation as compared to wild-type, and Class III, which has a total absence of amyloid formation as measured by our assays. By comparing the effect of the various mutations within these three classes, we attempted to elucidate the individual effect of each physiochemical property on amyloid formation.

Results

A variety of methods to monitor amyloid formation were used in this study. The primary method was a disappearance of monomer assay (DMA) that measured the chnge in monomer concentration over time by an FPLC. Thioflavin T (ThT) fluorescence, an amyloid specific fluorescent dye,[111-116] and electron microscopy (EM) were used to confirm amyloid formation since the disappearance of monomer assay could not distinguish fibril formation from other types of aggregation. All of these methods are discussed in more detail in Chapter III.

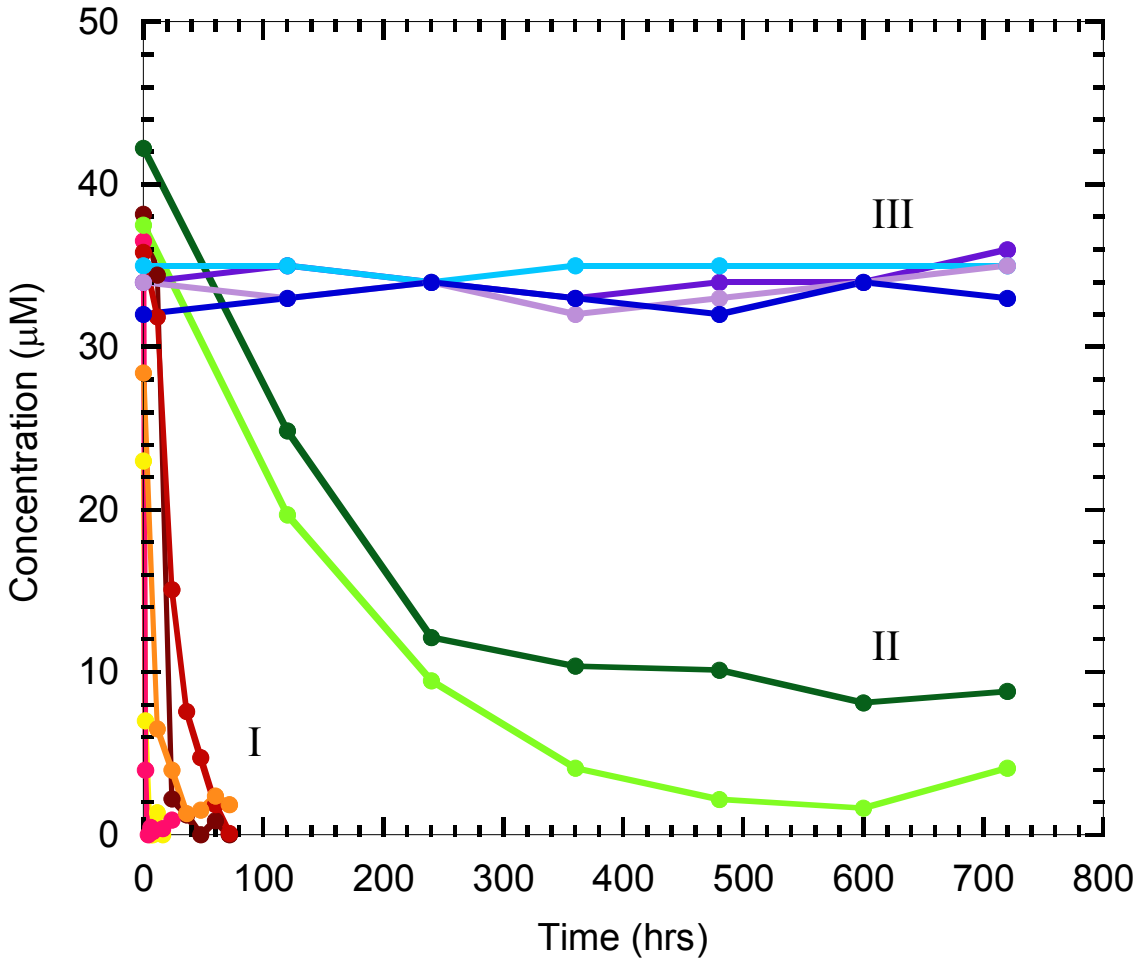

Figure 15. FPLC sedimentation data for selected Leu34 mutants of Aβ(25-35) at pH 4.8, 37°C. Class I variants are wild-type Aβ(25-35) (maroon), L34I (yellow), L34M (pink), L34Q (red), L34V (light orange). Class II mutants are L34C (light green) and L34E (dark green). Class III mutants are L34A (purple), L34K (light purple), L34P (cyan), and L34T (blue). Class I mutants are clustered around wild-type, Class II mutants have decreased aggregation, and Class III mutants show no aggregation after two months. Lines are used to guide the eye.

Aggregation of Leu34 mutants

Many of the Leu34 substitutions had a significant effect on amyloid formation (Fig. 15), and half of the peptides completely lost the ability to form fibrils. Of the 10 peptides that could aggregate, we saw distinct differences in fibril formation, namely in the final monomer concentration at equilibrium (critical concentration, or C_r) and the time needed to reach the concentration halfway to the Cr (halftime, or $t_{1/2}$) (Table 6).

Table 6. Amyloid formation data for Class I and Class II mutants

	C_r (μM)			$t_{1/2}$ (hrs)		
Peptide	pH 3.0	pH 4.8	pH 5.5	pH 3.0	pH 4.8	pH 5.5
Class I						
Aβ wt	0	0	0	126	19	6
L34F	IA	IA	IA	IA	IA	IA
L34I	0	0	IA	2	1	IA
L34M	7	0	0	12	2	1
L34Q	6	1	1	200	24	3
L34V	13	2	5	36	8	4
Class II						
L34C	NA	3	1	NA	240	94
L34E	NA	9	11	NA	396	242
L34G	NA	NA	24	NA	NA	260
L34S	NA	NA	16	NA	NA	360

Class determined by ability to form amyloid. 'IA' indicates immediate aggregation, therefore no data could be obtained. 'NA' indicates no aggregation. Errors are less than or equal to 10%

In fact, we observed such a distinct separation between the groups of peptides that we were able to easily divide the twenty peptides into three classes (Table 7). Class I peptides formed fibrils similarly to wild-type with comparable $t_{1/2}$ and C_r values, Class II mutants had significantly reduced aggregation that translated into larger $t_{1/2}$ and C_r

values than wild-type, and Class III mutants were unable to form fibrils for up to two months. For example, L34I, along with other Class I mutants such as L34M and L34Q

Table 7. Classification of peptides[a]

Class I	Class II	Class III
Aβ wt[b]	L34C[b]	L34A[b]
L34F[b]	L34E	L34D
L34I[b]	L34G	L34H
L34M[b]	L34S	L34K
L34Q		L34N
L34V[b]		L34P
		L34R
		L34T
		L34W[b]
		L34Y[b]

[a] Class determined by ability to form amyloid
[b] Predicted to β-aggregate by TANGO (Ref. 59)

did not have an appreciable difference in C_r or $t_{1/2}$ when compared to wild-type at pH 4.8 and pH 5.5 (Table 6). There were only observable differences at pH 3.0 where the peptides were fully ionized. At the higher pH values, all of the Class I mutants aggregated until little to no monomeric peptide was detected, and the aggregation took place typically within 24 hours, L34Q being the only exception. However, at the lower pH the slight variations observed at pH 4.8 and pH 5.5 were exaggerated, demonstrating a noticeable change in both the extent and speed of fibril formation. At pH 3.0, wild-type monomer was no longer detected at the end of the assay, but when compared to L34V, we saw a marked increase in the C_r to 13 μM for L34V. The $t_{1/2}$ values were also

distinctly different at pH 3.0. The $t_{1/2}$ of wild-type was 126 hours, while the $t_{1/2}$ for L34I was 2 hours, L34V was 36 hours, and L34Q was 200 hours. Even though the C_r values for many of these peptides are similar, the $t_{1/2}$ of each mutant thoroughly demonstrates variations in the kinetics of aggregation. One peptide of note was L34F; this mutant, along with L34I at pH 5.5, aggregated far too quickly for any meaningful measurement to be made, making it a Class I mutant.

With the four Class II mutants, the C_r and $t_{1/2}$ were both larger than wild-type at pH 4.8 and pH 5.5, though the most significant difference was found in the $t_{1/2}$ at both pH conditions (Table 6). The C_r of L34C at pH 4.8 was 3 μM, which was not significantly different than wild-type at that pH, where the monomer was no longer detectable. However, $t_{1/2}$ of L34C at pH 4.8 was 240 hours, which was clearly longer than the $t_{1/2}$ of wild-type, which was only 19 hours. It was a similar situation when comparing L34E to wild-type, where the $t_{1/2}$ at pH 4.8 of L34E was 396 hours, an even longer value compared to wild-type, while the C_r of L34E was 9 μM. These differences were smaller at pH 5.5; however, the $t_{1/2}$ of each peptide was still up to two orders of magnitude larger than wild-type. The last two Class II mutants were L34G and L34S, both of which were unable to form amyloid fibrils at any pH other than pH 5.5. Again, the $t_{1/2}$ values at this pH, 260 hours and 360 hours for L34G and L34S, respectively, were two orders of magnitude longer than wild-type. Although different than the other Class II mutants, L34G and L34S had significantly larger critical concentrations that were the two highest C_r values observed in this study.

As stated above, the Class III mutants did not form amyloid fibrils under any conditions that we explored up to several months. With a few Class III mutants such as L34A, L34K, and L34T, a large, unknown, amorphous aggregate was observed in the test tube; however, once run through an FPLC column, only monomeric peptide was detected. This is most likely due to the aggregate dissolving since the monomer concentration remained constant throughout the entire assay. Aggregates from L34K and L34T were also detected using dynamic light scattering (DLS), with the aggregate effective diameter being over 1.2 μm. We also tested several other Class III mutants for aggregation using DLS since L34K and L34T showed rather large aggregates. All of the Class III peptides had some aggregation, though the size ranged considerably, from 100 nm for L34D to approximately 1.3 μm for L34K (data not shown). The presence of these aggregates is similar to the loosely-associated aggregates that dissociate into monomer during the early stages of the aggregation process discussed in Chapter III.

Thioflavin T fluorescence

All of the Class I mutants were assayed with ThT and had confirmed amyloid formation. The precipitates from L34F and L34I at pH 5.5 were also tested, and were ThT positive, suggesting that the immediate aggregation was fibrillar. ThT fluorescence was used to confirm that the loss of monomer concentration of the Class II mutants was fibril formation, as with the Class I mutants. The Class III mutants were also tested and found to be negative by ThT fluorescence, including the aggregates found in L34A, L34K, and L34T samples.

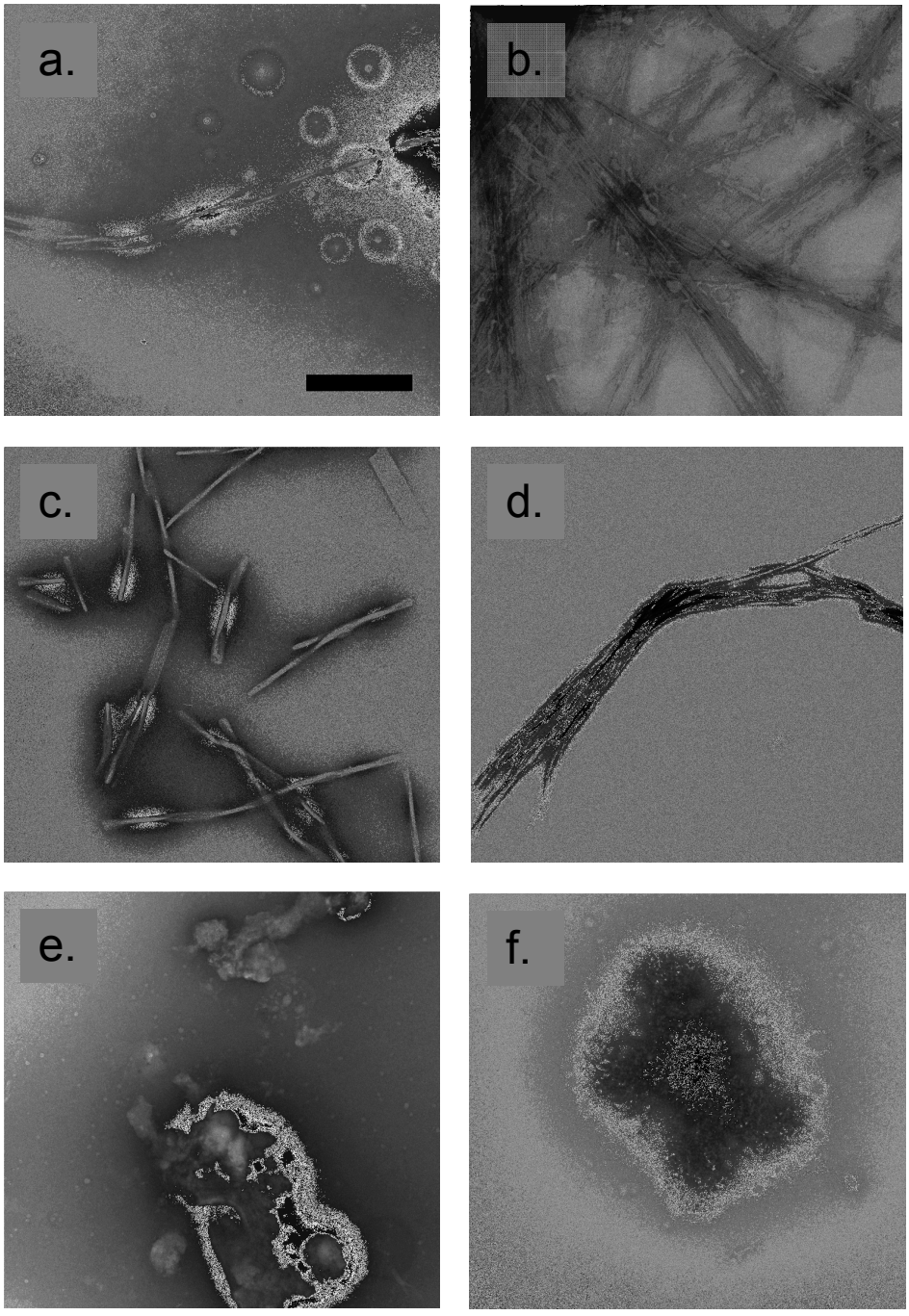

Figure 16. Electron micrographs of aged peptide samples with representations from each class of Leu34 variants. Class I variants represented are (a.) Aβ(25-35), (b.) L34I, and (c.) L34M. The Class II mutants is (d.) L34C. Class III mutants are (e.) L34D and (f.) L34P. Scale bar is 300 nm.

Electron microscopy

ThT is a useful test for amyloid formation, but for further confirmation, we utilized EM for ten of the twenty peptides, focusing on the Class I and Class II mutants. All of the peptides examined had varied fibril structure and size, despite identical aggregation conditions (Fig. 16). The wild-type peptide had long, thin, twisted fibrils over a μm long and 20 nm wide (Fig. 16a.), while L34I had fibrils of varying width, though averaging 20 nm, that stretched over a micron long that appeared mesh-like (Fig. 16b.). Another Class I mutant, L34M, had shorter, thicker twisted fibrils that ranged from 250-600 nm in length and 10-30 nm in width (Fig. 16c.). L34C, a Class II mutant, had straight, thick fibrils that clumped together and stretched over a micron in length and 10 nm in width (Fig. 16d.). The Class III mutants that we examined did not have fibrils, though several had amorphous aggregation (Figs. 16e. and 16f.).

Cytotoxicity studies

We selected fourteen peptides to use in our cytotoxicity studies with brain endothelial cells (Table 8). As observed previously, wild-type Aβ(25-35) was cytotoxic at concentrations of 25 μM and above, though not noticeably toxic at 10 μM.[106; 135; 136] Of the four Class I mutants studied (L34F, L34M, L34Q, and L34V), only L34V was cytotoxic at concentrations of 25 μM and above. The Class II mutants we studied were L34E, L34C, and L34S, and both L34E and L34S showed cytotoxicity at concentrations of 25 μM and above, though only L34S was also toxic at 10 μM. In addition to the peptides that formed amyloid, we decided to examine the Class III mutants as well,

specifically L34A, L34D, L34K, L34N, L34P, L34T, and L34Y. Interestingly, over half were cytotoxic. L34K was toxic at all concentrations, while L34A and L34T were both toxic at 50 μM. Also, L34N appeared to have a limited effect on cell survival at 50 μM, as well as L34D at 25 μM. The rest of the Class III mutants were found to have little to no cytotoxicity.

Table 8. Amyloid formation and cytotoxicity data of select mutants

	Amyloid	Cytotoxicity		
Peptide	formation	10 μM	25 μM	50 μM
Aβ wt	+	–	+	+
L34A	–	–	–	+
L34C	+	–	–	–
L34D	–	–	+	+
L34E	+	–	+	+
L34F	+	–	–	–
L34M	+	–	–	–
L34N	–	–	–	+
L34P	–	–	–	–
L34Q	+	–	–	–
L34S	+	+	+	+
L34T	–	–	–	+
L34V	+	–	+	+
L34W	–	–	–	–
L34Y	–	–	–	–

'+' indicates positive result. '–' indicates negative result.

Discussion

There are several physiochemical properties that have been implicated in amyloid formation, though there is still much debate on which properties are the most important.

This uncertainty is due, in part, to the vast differences in the types of peptides and proteins known to form fibrils, as well as the vast number of mutations made to these peptides in order to study aggregation. Because of this, we set out to study Aβ(25-35) and 19 variants of the Leu34 position of this peptide. The goal was to use this collection of peptides to distinguish which physiochemical properties were the most important. The properties of particular notice are: β-strand propensity, hydrophobicity, residue charge, and solubility. Other groups have substituted the naturally occurring amino acids into one position of other peptides, however, these studies did not study Met and Cys or took into account qualitative, biased results such as fibril morphology as judged by researchers.[28;32]

Distinct patterns in amyloid formation emerged between the Leu34 variants which made classification of the mutants relatively simple (Table 7). To further characterize the differences in aggregation, a handful of mutants were investigated at pH 4.8 (Fig. 15). Several mutants retained wild-type-like aggregation at all three pHs used in this study: pH 3.0 where the peptide had a +2 charge, pH 4.8 where the peptide had a net charge around +1, and pH 5.5 where the peptide net charge approached neutral. The mutants that could aggregate at all three pH conditions, we labeled as Class I mutants. Each Class I variant is expected to have a similar pI to wild-type; however the pIs were not measured. The peptides we categorized as Class II mutants had marked perturbation of amyloid formation and all had absence of amyloid formation at the lowest pH studied, and two of the Class II mutants had an absence of amyloid formation at pH 4.8 as well.

The Class II mutants also had reduced amyloid formation, leaving higher concentrations of monomeric peptide once aggregation was complete, and the aggregation process took significantly longer than the wild-type peptide. Some of the Class II and Class III mutants are expected to have a different pI compared to the wild-type peptide since charges are introduced in several cases. Interestingly, half of the peptides studied fell into Class III, which showed no apparent amyloid formation in any condition used for this study (Table 7). This demonstrated the sensitivity of position 34 in this peptide as well as how easily amyloidosis can be disrupted.

As mentioned above, the naturally occurring amino acids have been substituted into the full length Aβ(1-40)[28] and tau-related peptides.[32] Although these previous studies observed a continuum of amyloid formation between the variants instead of the distinct classes as shown here, the general aggregation trend between the amino acids was consistent. Class I amino acids such as Gln, Ile, Leu, Met, Phe, and Val were shown to be among the top amyloid forming amino acids.[28; 32] Also, Class III amino acids, Asp, His, Lys, and Pro, were found to be some of the worst amyloid forming amino acids. There was some disagreement over the amino acids of medium aggregation, i.e. those found in Class II; however, for the most part, the findings reported here appear to agree with previous studies.[28; 32]

Within the Class I mutants, we observed that the variant residues – Phe, Ile, Met, Gln, and Val – are all in the upper half of β-strand propensity scales, and in the lower half of

the solubility scale.[58; 141] These amino acids also introduced no charge to the peptide and all but Gln are more hydrophobic than Ala.[89] In previous studies, mutations within the full length Aβ from any of the Class I amino acids to Ala, Asp, Cys, Lys, Pro, or Ser have been shown to adversely affect amyloid formation.[28-31] The opposite effect has been observed when Class II or Class III amino acids were mutated to the Class I amino acids,[8; 28] demonstrating that Phe, Ile, Met, Gln, and Val are strongly amyloidogenic. Considering the physiochemical properties (Table 5) and past studies, our results were not surprising, except perhaps that Gln, which is a relatively hydrophilic residue, was present in the Class I mutants. However, upon examining the naturally occurring mutation that leads to the Dutch familial form of Alzheimer's disease (E22Q), a form that has an increase in aggregation propensity, perhaps mutating to Gln should show similar aggregation to wild-type as Gln is apparently perfectly capable of increasing amyloid formation.

After examining the Class I variants in relation to the Class II and Class III mutants, hydrophobicity appears to influence amyloid formation, as is often hypothesized in literature.[33; 45; 46; 54] When comparing the Class I variant, L34M, to L34C, a Class II variant, the only noteworthy difference in the physiochemical properties between Met and Cys is the higher hydrophobicity of Met (Table 5). Assuming that the increased hydrophobicity of the Met is seen in L34M, the enhanced fibrilogenesis observed with L34M as compared to L34C should be due to this change in hydrophobicity.

Further examination of the Class I mutants revealed the possible importance of β-strand propensity. When comparing Ile to Leu, all of the physiochemical properties we looked at, except β-strand propensity, are the same (Table 5). Ile has a higher β-strand propensity than Leu, and with that change, we saw a substantial increase in amyloid formation of L34I as compared to wild-type, most notably in the $t_{1/2}$ (Table 6). At pH 3.0, this difference was most pronounced when wild-type had a $t_{1/2}$ of 126 hours while L34I was 2 hours, a decrease of nearly two orders of magnitude from wild-type. This was supported by another study in Aβ(1-40) that reported an increase in the stability of the fibrils when mutating Val to Ile as opposed to Val to Leu.[28] At this point, the properties that appeared to have the most influence on fibril formation were hydrophobicity and β-strand propensity.

Among the Class II mutants, several of the substituted amino acids have a wide range of hydrophobicity, β-strand propensity, and solubility. Hydrophobicity and β-strand propensity values for the Class II amino acids were from the middle to the lower end of the two scales, and the solubility values were found in the middle to upper portion of that scale. Also, Glu introduced a charged residue into the L34E peptide. When examining these physiochemical properties, one would expect a substantial decrease in amyloidosis, which was supported by previous studies stating that mutating almost any other amino acid to a Class II amino acid discourages amyloid formation.[28; 29; 39] Previous studies similar to ours show that one or more of the Class II amino acids are mediocre amyloid formers, however there is significant disagreement between studies as to the amyloid

propensity of Cys, Glu, Gly, and Ser.[28; 32] As for this study, we assume various factors allowed these peptides to aggregate. For example, Ser has several properties the same as Gln,[89; 141] which is a Class I amino acid; however, Ser is more soluble than Gln[58] and L34S had a marked decrease in amyloid formation. This increased solubility could explain the decrease in fibril formation seen here and previously.[28] Also, this comparison suggests that solubility may be an important factor in amyloidosis.

The Arctic (E22G) and Flemish (A21G) variants of familial Alzheimer's disease support the data found from L34G since this mutant is still capable of forming amyloid fibrils despite the seemingly discouraging physiochemical properties of the Gly residue as compared to an amino acid such as Ala (Table 5). This was further supported by mutational studies that showed little to no change when mutating from a Val or Glu to a Gly as well as destabilizing effects from mutating a Gly to Ala, Cys, or Pro in Aβ(1-40).[8; 28-31] It is possible that the increased flexibility of the Gly allows for aggregation, though more likely is the steric benefits of an absent side group since many amyloidogenic peptides have residues with bulky side chains, i.e. Phe, Trp, and Tyr.

Overall, the Class III mutants were not expected to aggregate since many of the Class III amino acids, when compared to Leu, have low hydrophobicity, low β-strand propensity, high solubility, or are charged (Table 5). Also, several of the Class III amino acids have already been shown to inhibit aggregation to varying degrees in full length Aβ and tau-related peptides,[28; 30; 32; 39] which is consistent with our results. Therefore, it was

somewhat surprising to observe aggregation by DLS, though judging by the overall hydrophobic nature of the Aβ peptide in an aqueous environment, this aggregation might be expected in all of the Leu34 variants. However, these Class III mutants appear monomeric by FPLC. The likely explanation for this is that the aggregates were loosely associated and therefore disaggregated easily when passed through an FPLC column.

One Class III mutant of note was L34A. According to the physiochemical properties of Ala as compared to Gly (Table 5) and previous studies,[32; 39; 48; 65] L34A should have aggregated more than L34G, a Class II mutant; however, L34A appeared to have a total absence of fibril formation. Supporting data from a previous study was found from the naturally occurring A21G variant associated with Flemish familial Alzheimer's disease, which has a higher propensity to form amyloid.[8] Further data was found in Aβ(1-40) with A18G which showed an increase in the rate of aggregation,[8] as well as the destabilization of fibrils by mutating Gly to Ala,[31] and increased cell survival with Gly to Ala mutants.[142] Therefore, despite the physiochemical properties, one might expect L34G to be a better amyloid former than L34A, which was exactly what we found. This implied that the context of the residue is exerting an influence on amyloid formation as opposed to the physiochemical properties.

Two Class III mutants that gave unexpected results were L34W and L34Y, since Trp and Tyr have been shown to promote aggregation.[28; 32; 38; 39] Also, in β-2-microglobulin, mutating from Tyr to Ala, Glu, or Ser was shown to decrease the rate of fibrilization.[65]

Because of these previous studies, we anticipated that L34W and L34Y would be Class I variants, most likely better than wild-type given that the substituted amino acids are less soluble than Leu, are not charged, and have higher hydrophobicity and β-strand propensity than Leu (Table 5). However, that was not what we observed. There was no change in the concentration of monomer for L34W and L34Y for up to three months. Our best guess is that this lack of fibril formation is due to the sterically unfavorable, bulky side chains of Trp and Tyr.

By using ThT fluorescence and electron microscopy, we confirmed that the peptides that showed a disappearance of monomer concentration were, indeed, forming amyloid fibrils. We observed differences in ThT fluorescence signal which were most likely due to each peptide binding ThT dye with varying efficiency, a characteristic of ThT that has been previously shown.[114] The diversities in fibril appearance and size observed by EM were not as easily explained, however. These variations could be due to any number of reasons, although a recent study that examined the structural differences of Aβ(1-40) fibrils within the same sample suggested that amyloid formation gives rise to polymorphism simply because there are many different possible interactions within and between molecules.[143] This was the most likely explanation, compounded by the mutations at the Leu34 position, allowing an even more noticeable diversity in fibril structure seen here and in previous studies.[144; 145]

The cytotoxicity data was also interesting since half of the peptides that were found to be toxic were not able to form amyloid fibrils (Table 8). This supports the hypothesis that the early oligomers, not the fibrils, are responsible for cytotoxicity.[21-24; 26; 27] Upon examination, we noticed a trend among the cytotoxic peptides: all but the wild-type peptide and L34V had a soluble, β-strand disfavored amino acid at position 34. However, among the peptides that were not cytotoxic, we also noticed a peptide with a soluble, β-strand disfavored amino acid at position 34, specifically, L34Q. This trend was not unexpected, as we found low solubility and high β-strand propensity to encourage amyloid formation, and cytotoxicity was discovered to be more closely associated with the lack of amyloid formation. As to what this trend means for the study of amyloid formation and cell toxicity, is uncertain, though it does lend strong credence to the popular hypothesis that the oligomeric Aβ peptides are responsible for cell death, as opposed to the insoluble fibrils.[23-26]

As mentioned earlier, there are several ways of predicting aggregation, and in some cases amyloid formation. The methods from Dobson *et.al*. and Caflisch *et.al.* were discussed in Chapter I. However, there are also two internet-based programs that are commonly used: TANGO[59; 91] from the Serrano laboratory and Waltz from the Switch laboratory.[92; 93] Though these two programs are comparable, only Waltz claims to predict regions of a sequence with a propensity to form amyloid, while TANGO predicts β-aggregation, or aggregation in a β-strand conformation, not necessarily amyloid. Both

of these programs examine the physiochemical properties of the sequence and attempt to calculate the probability of aggregating.

For the Aβ(25-35) peptides, we analyzed the sequences with both programs and received vastly different results. According to Waltz, not a single peptide in this study should form fibrils, which was obviously not the case. Because of this, it appears that Waltz was not a good predictor of amyloid formation in this case.

TANGO, on the other hand, predicted six of the ten amyloid forming mutants (Table 7). The wild-type peptide was predicted to β-aggregate as well as L34A, L34C, L34F, L34I, L34M, L34V, L34W, and L34Y, with wild-type, L34F, L34I and L34V having the highest probabilities. The remaining eleven mutants were not predicted to β-aggregate, but were instead predicted to form β-turns. TANGO incorrectly predicted L34W and L34Y to β-aggregate, which was what we predicted would happen as well, judging by the prevalence of Trp and Tyr in amyloidogenic peptides. The only other mutant predicted to β-aggregate that was found to be a Class III mutant was L34A, which had a low probability of β-aggregating, and therefore was not very likely to form amyloid. L34Q also gave an interesting result for the reason stated above, simply put, many of the physiochemical properties of the Gln should discourage fibril formation. Overall, TANGO predicted fibril formation better than Waltz in this study.

To conclude, in this study we examined all twenty naturally occurring amino acids in the 34 position of Aβ(25-35), and divided the peptides into three different classes. Class I retained wild-type-like fibril formation, Class II had significantly reduced amyloid formation, and Class III had an apparent loss of aggregation. Using these mutants, we determined the relative importance of four physiochemical properties and found the three to have the largest effect on amyloid formation were hydrophobicity, solubility, and β-strand propensity. This was a unique discovery as solubility is often overlooked in studies attempting to determine the effect of physiochemical properties on amyloidosis. We also observed that only half of the amyloid-forming peptides examined were cytotoxic, and that several variants which were unable to form fibrils yet formed aggregates detectable by DLS were cytotoxic. This supports the popular hypothesis that early oligomers are the toxic species.[21-24; 26; 27]

CHAPTER VI

SUMMARY

Here, a fragment of Aβ(1-42), the Alzheimer's peptide, was utilized to examine various aspects of amyloid formation. Aβ(25-35) was a useful model since there were no long-range interactions or higher order structure to contend with, yet the eleven residue fragment could still form fibrils similar to the full length Aβ(1-42) and was still cytotoxic. Using Aβ(25-35), this study attempted to contribute to a greater understanding of the process of amyloid formation and the properties that contribute to fibrilogenesis. The former was addressed by studying the step by step progression of aggregation, and the latter by determining the critical amyloidogenic region of Aβ(25-35) and the physiochemical properties that influenced fibril formation.

The stepped process of aggregation as well as the core of amyloid formation and the physiochemical properties that encourage amyloidosis were examined. Studies were performed at 37°C at pH 3, pH 4.8, or pH 5.5; the multiple pH conditions were necessary to control the charge of the Aβ(25-35) peptide, since charge affects amyloid formation. Also, a variety of methods were utilized in order to maximize the information gleaned regarding fibrilogenesis, among these were a disappearance of monomer assay (DMA), dynamic light scattering (DLS), Thioflavin T (ThT) fluorescence, and electron microscopy (EM). From these tests, differences in aggregation between the variants could be detected and conclusions could be made.

By studying the process of fibril formation using methods that could identify the steps of aggregation, we were able to follow the progression of monomeric peptide forming small, spherical oligomers, then chains of oligomers that flatten into sheets that later roll up into tubes. We believe these tubes mature into the amyloid fibrils found in the tissues of patients with the disease. Of note is that we observe two macrooligomeric species after this point in the process, namely twisted sheets and crystal-like plates. This study provided evidence for new supermolecular species which would not have been measured without the use of each of the four methods listed above.

It was also discovered that Aβ(30-35) is the critical region of Aβ(25-35) and is quite possibly the initiation point of aggregation. Aβ(30-35) was able to form fibrils like the longer Aβ(25-35) peptide, and through Ala scanning mutagenesis, residues 30-35 were all found to be important to amyloidosis since mutating any residue to Ala had a profound effect on aggregation. While G33A was able to form fibrils faster than wild-type Aβ(30-35), mutating any other residue to an Ala resulted in a total loss of amyloid formation. Also, we studied the cytotoxicity of each peptide and found that interestingly, Aβ(30-35), while able to form fibrils, was not found to be harmful to rat or mouse brain endothelial cells, but all of the mutants of this peptide were found to be toxic, showing a vast discrepancy in the association of fibrilogenesis and cytotoxicity.

Another important conclusion from our studies was that β-strand propensity and solubility have the largest effect on Aβ(25-35) amyloid formation. By inserting all

twenty naturally occurring amino acids into the Leu34 position of Aβ(25-35) and studying the aggregation of each mutant, we were able to divide the twenty peptides into three classes. Class I had wild-type like aggregation properties, Class II had severely diminished aggregation, and Class III displayed no aggregation up to two months. After measuring the aggregation of each peptide, we compared the physiochemical properties of each amino acid in position 34 and the corresponding amyloid formation data, discovering that β-strand propensity and solubility had the most influence on amyloidosis.

These individual studies have all provided interesting findings, but more work must still be done. Not the least of which is to repeat the studies of the stepped process and effect of physiochemical properties on amyloidosis using other amyloidogenic peptides to verify our results. It cannot be assumed that other peptides or proteins would have the same intermediate species in the amyloid formation pathway. Neither can it be assumed that a peptide that is more hydrophilic or less likely to form a β-strand than Aβ would demonstrate that solubility and β-strand propensity are the most important physiochemical properties. Also, the specific molecular structure of any intermediates found in the course of any future study should be investigated since that should provide another insight into the aggregation process. However, despite this need for further confirmation, all of these findings will hopefully contribute to a better understanding not only of the process of amyloid formation, but also the causes of this disease-associated aggregation.

REFERENCES

1. Alzheimer, A. (1907). Uber eine eigenartige Erkrankung der Hirnrinde. *Allgemeine Zeitschrift fur Psychiatrie und Psychisch-Gerichtliche Medizine* **64**, 146-148.
2. Association, A. (2009). 2009 Alzheimer's disease facts and figures. *Alzheimers Dement.* **5**, 234-270.
3. Sipe, J. D. & Cohen, A. S. (2000). Review: history of the amyloid fibril. *J. Struct. Biol.* **130**, 88-98.
4. LaFerla, F. M., Green, K. N. & Oddo, S. (2007). Intracellular amyloid-beta in Alzheimer's disease. *Nat. Rev. Neurosci.* **8**, 499-509.
5. Ballatore, C., Lee, V. M. & Trojanowski, J. Q. (2007). Tau-mediated neurodegeneration in Alzheimer's disease and related disorders. *Nat. Rev. Neurosci.* **8**, 663-672.
6. Caltagarone, J., Jing, Z. & Bowser, R. (2007). Focal adhesions regulate Abeta signaling and cell death in Alzheimer's disease. *Biochim. Biophys. Acta* **1772**, 438-445.
7. Grant, M. A., Lazo, N. D., Lomakin, A., Condron, M. M., Arai, H., Yamin, G., Rigby, A. C. & Teplow, D. B. (2007). Familial Alzheimer's disease mutations alter the stability of the amyloid beta-protein monomer folding nucleus. *Proc. Natl. Acad. Sci. USA* **104**, 16522-16527.
8. Meinhardt, J., Tartaglia, G. G., Pawar, A., Christopeit, T., Hortschansky, P., Schroeckh, V., Dobson, C. M., Vendruscolo, M. & Fandrich, M. (2007).

Similarities in the thermodynamics and kinetics of aggregation of disease-related Abeta(1-40) peptides. *Protein Sci.* **16**, 1214-1222.

9. Haass, C., Lemere, C. A., Capell, A., Citron, M., Seubert, P., Schenk, D., Lannfelt, L. & Selkoe, D. J. (1995). The Swedish mutation causes early-onset Alzheimer's disease by beta-secretase cleavage within the secretory pathway. *Nat. Med.* **1**, 1291-1296.

10. Nilsberth, C., Westlind-Danielsson, A., Eckman, C. B., Condron, M. M., Axelman, K., Forsell, C., Stenh, C., Luthman, J., Teplow, D. B., Younkin, S. G., Naslund, J. & Lannfelt, L. (2001). The 'Arctic' APP mutation (E693G) causes Alzheimer's disease by enhanced Abeta protofibril formation. *Nat. Neurosci.* **4**, 887-893.

11. Sorbi, S., Nacmias, B., Mortilla, M., Forleo, P., Piacentini, S. & Amaducci, L. (1994). Molecular genetics of Alzheimer's disease in Italian families. *Neurochem. Int.* **25**, 81-84.

12. Gyure, K. A., Durham, R., Stewart, W. F., Smialek, J. E. & Troncoso, J. C. (2001). Intraneuronal abeta-amyloid precedes development of amyloid plaques in Down syndrome. *Arch. Pathol. Lab. Med.* **125**, 489-492.

13. Lemere, C. A., Grenfell, T. J. & Selkoe, D. J. (1999). The AMY antigen co-occurs with abeta and follows its deposition in the amyloid plaques of Alzheimer's disease and down syndrome. *Am. J. Pathol.* **155**, 29-37.

14. Shankar, G. M., Li, S., Mehta, T. H., Garcia-Munoz, A., Shepardson, N. E., Smith, I., Brett, F. M., Farrell, M. A., Rowan, M. J., Lemere, C. A., Regan, C.

M., Walsh, D. M., Sabatini, B. L. & Selkoe, D. J. (2008). Amyloid-beta protein dimers isolated directly from Alzheimer's brains impair synaptic plasticity and memory. *Nat. Med.* **14**, 837-842.

15. Lin, H., Bhatia, R. & Lal, R. (2001). Amyloid beta protein forms ion channels: implications for Alzheimer's disease pathophysiology. *FASEB J.* **15**, 2433-2444.

16. Wright, S., Malinin, N. L., Powell, K. A., Yednock, T., Rydel, R. E. & Griswold-Prenner, I. (2007). Alpha2beta1 and alphaVbeta1 integrin signaling pathways mediate amyloid-beta-induced neurotoxicity. *Neurobiol. Aging,* **28**, 226-237.

17. Chimon, S., Shaibat, M. A., Jones, C. R., Calero, D. C., Aizezi, B. & Ishii, Y. (2007). Evidence of fibril-like beta-sheet structures in a neurotoxic amyloid intermediate of Alzheimer's beta-amyloid. *Nat. Struct. Mol. Biol.* **14**, 1157-1164.

18. Pike, C. J., Walencewicz-Wasserman, A. J., Kosmoski, J., Cribbs, D. H., Glabe, C. G. & Cotman, C. W. (1995). Structure-activity analyses of beta-amyloid peptides: contributions of the beta 25-35 region to aggregation and neurotoxicity. *J. Neurochem.* **64**, 253-265.

19. Knobloch, M., Konietzko, U., Krebs, D. C. & Nitsch, R. M. (2007). Intracellular Abeta and cognitive deficits precede beta-amyloid deposition in transgenic arcAbeta mice. *Neurobiol. Aging,* **28**, 1297-1306.

20. Tsunekawa, H., Noda, Y., Mouri, A., Yoneda, F. & Nabeshima, T. (2008). Synergistic effects of selegiline and donepezil on cognitive impairment induced by amyloid beta (25-35). *Behav. Brain Res.* **190**, 224-232.

21. McLean, C. A., Cherny, R. A., Fraser, F. W., Fuller, S. J., Smith, M. J., Beyreuther, K., Bush, A. I. & Masters, C. L. (1999). Soluble pool of Abeta amyloid as a determinant of severity of neurodegeneration in Alzheimer's disease. *Ann. Neurol.* **46**, 860-866.

22. Lue, L. F., Kuo, Y. M., Roher, A. E., Brachova, L., Shen, Y., Sue, L., Beach, T., Kurth, J. H., Rydel, R. E. & Rogers, J. (1999). Soluble amyloid beta peptide concentration as a predictor of synaptic change in Alzheimer's disease. *Am. J. Pathol.* **155**, 853-862.

23. Barghorn, S., Nimmrich, V., Striebinger, A., Krantz, C., Keller, P., Janson, B., Bahr, M., Schmidt, M., Bitner, R. S., Harlan, J., Barlow, E., Ebert, U. & Hillen, H. (2005). Globular amyloid beta-peptide oligomer - a homogenous and stable neuropathological protein in Alzheimer's disease. *J. Neurochem.* **95**, 834-847.

24. Kuo, Y. M., Emmerling, M. R., Vigo-Pelfrey, C., Kasunic, T. C., Kirkpatrick, J. B., Murdoch, G. H., Ball, M. J. & Roher, A. E. (1996). Water-soluble Abeta (N-40, N-42) oligomers in normal and Alzheimer disease brains. *J. Biol. Chem.* **271**, 4077-4081.

25. Lansbury, P. T. & Lashuel, H. A. (2006). A century-old debate on protein aggregation and neurodegeneration enters the clinic. *Nature,* **443**, 774-779.

26. Vieira, M. N., Forny-Germano, L., Saraiva, L. M., Sebollela, A., Martinez, A. M., Houzel, J. C., De Felice, F. G. & Ferreira, S. T. (2007). Soluble oligomers from a non-disease related protein mimic Abeta-induced tau hyperphosphorylation and neurodegeneration. *J. Neurochem.* **103**, 736-748.

27. Cheng, I. H., Scearce-Levie, K., Legleiter, J., Palop, J. J., Gerstein, H., Bien-Ly, N., Puolivali, J., Lesne, S., Ashe, K. H., Muchowski, P. J. & Mucke, L. (2007). Accelerating amyloid-beta fibrillization reduces oligomer levels and functional deficits in Alzheimer disease mouse models. *J. Biol. Chem.* **282**, 23818-23828.

28. Hortschansky, P., Christopeit, T., Schroeckh, V. & Fandrich, M. (2005). Thermodynamic analysis of the aggregation propensity of oxidized Alzheimer's beta-amyloid variants. *Protein Sci.* **14**, 2915-2918.

29. Shivaprasad, S. & Wetzel, R. (2006). Scanning cysteine mutagenesis analysis of Abeta-(1-40) amyloid fibrils. *J. Biol. Chem.* **281**, 993-1000.

30. Williams, A. D., Portelius, E., Kheterpal, I., Guo, J. T., Cook, K. D., Xu, Y. & Wetzel, R. (2004). Mapping abeta amyloid fibril secondary structure using scanning proline mutagenesis. *J. Mol. Biol.* **335**, 833-842.

31. Williams, A. D., Shivaprasad, S. & Wetzel, R. (2006). Alanine scanning mutagenesis of Abeta(1-40) amyloid fibril stability. *J. Mol. Biol.* **357**, 1283-1294.

32. Rojas Quijano, F. A., Morrow, D., Wise, B. M., Brancia, F. L. & Goux, W. J. (2006). Prediction of nucleating sequences from amyloidogenic propensities of tau-related peptides. *Biochemistry,* **45**, 4638-4652.

33. Calamai, M., Taddei, N., Stefani, M., Ramponi, G. & Chiti, F. (2003). Relative influence of hydrophobicity and net charge in the aggregation of two homologous proteins. *Biochemistry,* **42**, 15078-15083.

34. Chiti, F., Taddei, N., Baroni, F., Capanni, C., Stefani, M., Ramponi, G. & Dobson, C. M. (2002). Kinetic partitioning of protein folding and aggregation. *Nat. Struct. Biol.* **9**, 137-43.

35. Fei, L. & Perrett, S. (2009). Disulfide bond formation significantly accelerates the assembly of Ure2p fibrils because of the proximity of a potential amyloid stretch. *J. Biol. Chem.* **284**, 11134-11141.

36. Christopeit, T., Hortschansky, P., Schroeckh, V., Guhrs, K., Zandomeneghi, G. & Fandrich, M. (2005). Mutagenic analysis of the nucleation propensity of oxidized Alzheimer's beta-amyloid peptide. *Protein Sci.* **14**, 2125-2131.

37. Calamai, M., Tartaglia, G. G., Vendruscolo, M., Chiti, F. & Dobson, C. M. (2009). Mutational analysis of the aggregation-prone and disaggregation-prone regions of acylphosphatase. *J. Mol. Biol.* **387**, 965-974.

38. Bemporad, F., Taddei, N., Stefani, M. & Chiti, F. (2006). Assessing the role of aromatic residues in the amyloid aggregation of human muscle acylphosphatase. *Protein Sci.* **15**, 862-870.

39. Kim, W. & Hecht, M. H. (2005). Sequence determinants of enhanced amyloidogenicity of Alzheimer A{beta}42 peptide relative to A{beta}40. *J. Biol. Chem.* **280**, 35069-35076.

40. Kim, W. & Hecht, M. H. (2006). Generic hydrophobic residues are sufficient to promote aggregation of the Alzheimer's Abeta42 peptide. *Proc. Natl. Acad. Sci. USA,* **103**, 15824-15829.

41. Tjernberg, L., Hosia, W., Bark, N., Thyberg, J. & Johansson, J. (2002). Charge attraction and beta propensity are necessary for amyloid fibril formation from tetrapeptides. *J. Biol. Chem.* **277**, 43243-43246.

42. Zibaee, S., Jakes, R., Fraser, G., Serpell, L. C., Crowther, R. A. & Goedert, M. (2007). Sequence determinants for amyloid fibrillogenesis of human alpha-synuclein. *J. Mol. Biol.* **374**, 454-464.

43. Wurth, C., Guimard, N. K. & Hecht, M. H. (2002). Mutations that reduce aggregation of the Alzheimer's Abeta42 peptide: an unbiased search for the sequence determinants of Abeta amyloidogenesis. *J. Mol. Biol.* **319**, 1279-1290.

44. Chiti, F., Calamai, M., Taddei, N., Stefani, M., Ramponi, G. & Dobson, C. M. (2002). Studies of the aggregation of mutant proteins in vitro provide insights into the genetics of amyloid diseases. *Proc. Natl. Acad. Sci. USA,* **99 Suppl 4**, 16419-16426.

45. Chiti, F., Stefani, M., Taddei, N., Ramponi, G. & Dobson, C. M. (2003). Rationalization of the effects of mutations on peptide and protein aggregation rates. *Nature* **424**, 805-808.

46. Dyson, H. J., Wright, P. E. & Scheraga, H. A. (2006). The role of hydrophobic interactions in initiation and propagation of protein folding. *Proc. Natl. Acad. Sci. USA,* **103**, 13057-13061.

47. Pasquato, N., Berni, R., Folli, C., Alfieri, B., Cendron, L. & Zanotti, G. (2007). Acidic pH-induced conformational changes in amyloidogenic mutant transthyretin. *J. Mol. Biol.* **366**, 711-719.

48. Pawar, A. P., Dubay, K. F., Zurdo, J., Chiti, F., Vendruscolo, M. & Dobson, C. M. (2005). Prediction of "aggregation-prone" and "aggregation-susceptible" regions in proteins associated with neurodegenerative diseases. *J. Mol. Biol.* **350**, 379-392.

49. Raman, B., Chatani, E., Kihara, M., Ban, T., Sakai, M., Hasegawa, K., Naiki, H., Rao Ch, M. & Goto, Y. (2005). Critical balance of electrostatic and hydrophobic interactions is required for beta 2-microglobulin amyloid fibril growth and stability. *Biochemistry,* **44**, 1288-1299.

50. Schmittschmitt, J. P. & Scholtz, J. M. (2003). The role of protein stability, solubility, and net charge in amyloid fibril formation. *Protein Sci.* **12**, 2374-2378.

51. Tartaglia, G. G., Cavalli, A., Pellarin, R. & Caflisch, A. (2004). The role of aromaticity, exposed surface, and dipole moment in determining protein aggregation rates. *Protein Sci.* **13**, 1939-1941.

52. Tartaglia, G. G., Cavalli, A., Pellarin, R. & Caflisch, A. (2005). Prediction of aggregation rate and aggregation-prone segments in polypeptide sequences. *Protein Sci.* **14**, 2723-2734.

53. Wang, W. & Hecht, M. H. (2002). Rationally designed mutations convert de novo amyloid-like fibrils into monomeric beta-sheet proteins. *Proc. Natl. Acad. Sci. USA,* **99**, 2760-2765.

54. DuBay, K. F., Pawar, A. P., Chiti, F., Zurdo, J., Dobson, C. M. & Vendruscolo, M. (2004). Prediction of the absolute aggregation rates of amyloidogenic polypeptide chains. *J. Mol. Biol.* **341**, 1317-1326.

55. O'Nuallain, B., Shivaprasad, S., Kheterpal, I. & Wetzel, R. (2005). Thermodynamics of A beta(1-40) amyloid fibril elongation. *Biochemistry* **44**, 12709-12718.

56. Kim, W. & Hecht, M. H. (2008). Mutations enhance the aggregation propensity of the Alzheimer's A beta peptide. *J. Mol. Biol.* **377**, 565-574.

57. Chen, S., Ferrone, F. A. & Wetzel, R. (2002). Huntington's disease age-of-onset linked to polyglutamine aggregation nucleation. *Proc. Natl. Acad. Sci. USA* **99**, 11884-11889.

58. Trevino, S. R., Scholtz, J. M. & Pace, C. N. (2007). Amino acid contribution to protein solubility: Asp, Glu, and Ser contribute more favorably than the other hydrophilic amino acids in RNase Sa. *J. Mol. Biol.* **366**, 449-460.

59. Fernandez-Escamilla, A. M., Rousseau, F., Schymkowitz, J. & Serrano, L. (2004). Prediction of sequence-dependent and mutational effects on the aggregation of peptides and proteins. *Nat. Biotechnol.* **22**, 1302-1306.

60. Kallberg, Y., Gustafsson, M., Persson, B., Thyberg, J. & Johansson, J. (2001). Prediction of amyloid fibril-forming proteins. *J. Biol. Chem.* **276**, 12945-12950.

61. Yamaguchi, K., Matsumoto, T. & Kuwata, K. (2008). Critical region for amyloid fibril formation of mouse prion protein: unusual amyloidogenic properties of the helix 2 peptide. *Biochemistry* **47**, 13242-13251.

62. Picotti, P., De Franceschi, G., Frare, E., Spolaore, B., Zambonin, M., Chiti, F., de Laureto, P. P. & Fontana, A. (2007). Amyloid fibril formation and disaggregation

of fragment 1-29 of Apomyoglobin: insights into the effect of pH on protein fibrillogenesis. *J. Mol. Biol.* **367**, 1237-1245.

63. Gazit, E. (2002). A possible role for pi-stacking in the self-assembly of amyloid fibrils. *FASEB J.* **16**, 77-83.

64. Makin, O. S., Atkins, E., Sikorski, P., Johansson, J. & Serpell, L. C. (2005). Molecular basis for amyloid fibril formation and stability. *Proc. Natl. Acad. Sci. USA,* **102**, 315-320.

65. Platt, G. W., Routledge, K. E., Homans, S. W. & Radford, S. E. (2008). Fibril growth kinetics reveal a region of beta2-microglobulin important for nucleation and elongation of aggregation. *J. Mol. Biol.* **378**, 251-263.

66. Binger, K. J., Griffin, M. D. & Howlett, G. J. (2008). Methionine oxidation inhibits assembly and promotes disassembly of apolipoprotein C-II amyloid fibrils. *Biochemistry,* **47**, 10208-10217.

67. Clementi, M. E., Marini, S., Coletta, M., Orsini, F., Giardina, B. & Misiti, F. (2005). Abeta(31-35) and Abeta(25-35) fragments of amyloid beta-protein induce cellular death through apoptotic signals: role of the redox state of methionine-35. *FEBS Lett.* **579**, 2913-2918.

68. Hou, L., Kang, I., Marchant, R. E. & Zagorski, M. G. (2002). Methionine 35 oxidation reduces fibril assembly of the amyloid abeta-(1-42) peptide of Alzheimer's disease. *J. Biol. Chem.* **277**, 40173-40176.

69. Bitan, G., Tarus, B., Vollers, S. S., Lashuel, H. A., Condron, M. M., Straub, J. E. & Teplow, D. B. (2003). A molecular switch in amyloid assembly: Met35 and amyloid beta-protein oligomerization. *J. Am. Chem. Soc.* **125**, 15359-15365.

70. Misiti, F., Sampaolese, B., Pezzotti, M., Marini, S., Coletta, M., Ceccarelli, L., Giardina, B. & Clementi, M. E. (2005). Abeta(31-35) peptide induce apoptosis in PC 12 cells: contrast with Abeta(25-35) peptide and examination of underlying mechanisms. *Neurochem. Int.* **46**, 575-583.

71. Ricchelli, F., Buggio, R., Drago, D., Salmona, M., Forloni, G., Negro, A., Tognon, G. & Zatta, P. (2006). Aggregation/fibrillogenesis of recombinant human prion protein and Gerstmann-Straussler-Scheinker disease peptides in the presence of metal ions. *Biochemistry,* **45**, 6724-6732.

72. Salmona, M., Morbin, M., Massignan, T., Colombo, L., Mazzoleni, G., Capobianco, R., Diomede, L., Thaler, F., Mollica, L., Musco, G., Kourie, J. J., Bugiani, O., Sharma, D., Inouye, H., Kirschner, D. A., Forloni, G. & Tagliavini, F. (2003). Structural properties of Gerstmann-Straussler-Scheinker disease amyloid protein. *J. Biol. Chem.* **278**, 48146-48153.

73. Broome, B. M. & Hecht, M. H. (2000). Nature disfavors sequences of alternating polar and non-polar amino acids: implications for amyloidogenesis. *J. Mol. Biol.* **296**, 961-968.

74. Mandel-Gutfreund, Y. & Gregoret, L. M. (2002). On the significance of alternating patterns of polar and non-polar residues in beta-strands. *J. Mol. Biol.* **323**, 453-461.

75. West, M. W., Wang, W., Patterson, J., Mancias, J. D., Beasley, J. R. & Hecht, M. H. (1999). De novo amyloid proteins from designed combinatorial libraries. *Proc. Natl. Acad. Sci. USA,* **96**, 11211-11216.

76. Xiong, H., Buckwalter, B. L., Shieh, H. M. & Hecht, M. H. (1995). Periodicity of polar and nonpolar amino acids is the major determinant of secondary structure in self-assembling oligomeric peptides. *Proc. Natl. Acad. Sci. USA,* **92**, 6349-6353.

77. Klement, K., Wieligmann, K., Meinhardt, J., Hortschansky, P., Richter, W. & Fandrich, M. (2007). Effect of different salt ions on the propensity of aggregation and on the structure of Alzheimer's abeta(1-40) amyloid fibrils. *J. Mol. Biol.* **373**, 1321-1333.

78. Lee, S., Fernandez, E. J. & Good, T. A. (2007). Role of aggregation conditions in structure, stability, and toxicity of intermediates in the Abeta fibril formation pathway. *Protein Sci.* **16**, 723-732.

79. Moore, R. A., Hayes, S. F., Fischer, E. R. & Priola, S. A. (2007). Amyloid formation via supramolecular peptide assemblies. *Biochemistry,* **46**, 7079-7087.

80. Paravastu, A. K., Qahwash, I., Leapman, R. D., Meredith, S. C. & Tycko, R. (2009). Seeded growth of beta-amyloid fibrils from Alzheimer's brain-derived fibrils produces a distinct fibril structure. *Proc. Natl. Acad. Sci. USA,* **106**, 7443-7448.

81. Sasahara, K., Naiki, H. & Goto, Y. (2006). Exothermic effects observed upon heating of beta2-microglobulin monomers in the presence of amyloid seeds. *Biochemistry,* **45**, 8760-8769.

82. Sasahara, K., Yagi, H., Naiki, H. & Goto, Y. (2007). Heat-induced conversion of beta(2)-microglobulin and hen egg-white lysozyme into amyloid fibrils. *J. Mol. Biol.* **372**, 981-991.

83. Slepko, N., Bhattacharyya, A. M., Jackson, G. R., Steffan, J. S., Marsh, J. L., Thompson, L. M. & Wetzel, R. (2006). Normal-repeat-length polyglutamine peptides accelerate aggregation nucleation and cytotoxicity of expanded polyglutamine proteins. *Proc. Natl. Acad. Sci. USA,* **103**, 14367-14372.

84. Wood, S. J., Maleeff, B., Hart, T. & Wetzel, R. (1996). Physical, morphological and functional differences between ph 5.8 and 7.4 aggregates of the Alzheimer's amyloid peptide Abeta. *J. Mol. Biol.* **256**, 870-877.

85. Chiti, F., Webster, P., Taddei, N., Clark, A., Stefani, M., Ramponi, G. & Dobson, C. M. (1999). Designing conditions for in vitro formation of amyloid protofilaments and fibrils. *Proc. Natl. Acad. Sci. USA,* **96**, 3590-3594.

86. Litvinovich, S. V., Brew, S. A., Aota, S., Akiyama, S. K., Haudenschild, C. & Ingham, K. C. (1998). Formation of amyloid-like fibrils by self-association of a partially unfolded fibronectin type III module. *J. Mol. Biol.* **280**, 245-258.

87. Guijarro, J. I., Sunde, M., Jones, J. A., Campbell, I. D. & Dobson, C. M. (1998). Amyloid fibril formation by an SH3 domain. *Proc. Natl. Acad. Sci. USA,* **95**, 4224-4228.

88. Ramirez-Alvarado, M., Merkel, J. S. & Regan, L. (2000). A systematic exploration of the influence of the protein stability on amyloid fibril formation in vitro. *Proc. Natl. Acad. Sci. USA,* **97**, 8979-8984.

89. Roseman, M. A. (1988). Hydrophilicity of polar amino acid side-chains is markedly reduced by flanking peptide bonds. *J. Mol. Biol.* **200**, 513-522.

90. Koehl, P. & Levitt, M. (1999). Structure-based conformational preferences of amino acids. *Proc. Natl. Acad. Sci. USA,* **96**, 12524-12529.

91. Fernandez, A., Rousseau, F., Schymkowitz, J. & Serrano, L. (2004). TANGO. Prediction data. http://tango.crg.es/ (accessed on January 5, 2009).

92. Reumers, J., Conde, L., Medina, I., Maurer-Stroh, S., Van Durme, J., Dopazo, J., Rousseau, F. & Schymkowitz, J. (2008). Joint annotation of coding and non-coding single nucleotide polymorphisms and mutations in the SNPeffect and PupaSuite databases. *Nucleic Acids Res.* **36**, D825-829.

93. Switch laboratory (2008). Waltz. Prediction data. http://wsitpc7.vub.ac.be/cgi-bin/submit.egi (accessed on January 5, 2009).

94. Burdick, D., Soreghan, B., Kwon, M., Kosmoski, J., Knauer, M., Henschen, A., Yates, J., Cotman, C. & Glabe, C. (1992). Assembly and aggregation properties of synthetic Alzheimer's A4/beta amyloid peptide analogs. *J. Biol. Chem.* **267**, 546-554.

95. O'Nuallain, B., Thakur, A. K., Williams, A. D., Bhattacharyya, A. M., Chen, S., Thiagarajan, G. & Wetzel, R. (2006). Kinetics and thermodynamics of amyloid

assembly using a high-performance liquid chromatography-based sedimentation assay. *Methods Enzymol.* **413**, 34-74.

96. Sapatino, B. V., Welsh, C. J., Smith, C. A., Bebo, B. F. & Linthicum, D. S. (1993). Cloned mouse cerebrovascular endothelial cells that maintain their differentiation markers for factor VIII, low density lipoprotein, and angiotensin-converting enzyme. *In Vitro Cell Dev. Biol. Anim.* **29A**, 923-928.

97. Su, Y. & Chang, P. T. (2001). Acidic pH promotes the formation of toxic fibrils from beta-amyloid peptide. *Brain Res.* **893**, 287-291.

98. Jarrett, J. T. & Lansbury, P. T. (1993). Seeding "one-dimensional crystallization" of amyloid: A pathogenic mechanism in Alzheimer's disease and scrapie? *Cell,* **73**, 1055-1058.

99. Kelly, J. W. (2000). Mechanisms of amyloidogenesis. *Nat. Struct. Mol. Biol.* **7**, 824-826.

100. Roychaudhuri, R., Yang, M., Hoshi, M. M. & Teplow, D. B. (2009). Amyloid {beta}-Protein Assembly and Alzheimer Disease. *J. Biol. Chem.* **284**, 4749-4753.

101. Terry, R. D., Masliah, E., Salmon, D. P., Butters, N., DeTeresa, R., Hill, R., Hansen, L. A. & Katzman, R. (1991). Physical basis of cognitive alterations in Alzheimer's disease: synapse loss is the major correlate of cognitive impairment. *Ann. Neurol.* **30**, 572-580.

102. Boland, K., Behrens, M., Choi, D., Manias, K. & Perlmutter, D. H. (1996). The serpin-enzyme complex receptor recognizes soluble, nontoxic amyloid-beta

peptide but not aggregated, cytotoxic amyloid-beta peptide. *J. Biol. Chem.* **271**, 18032-18044.

103. Egashira, N., Iwasaki, K., Akiyoshi, Y., Takagaki, Y., Hatip-Al-Khatib, I., Mishima, K., Kurauchi, K., Ikeda, T. & Fujiwara, M. (2005). Protective effect of Toki-shakuyaku-san on amyloid beta25-35-induced neuronal damage in cultured rat cortical neurons. *Phytother. Res.* **19**, 450-453.

104. Giunta, S., Galeazzi, R., Valli, M. B., Corder, E. H. & Galeazzi, L. (2004). Transferrin neutralization of amyloid beta 25-35 cytotoxicity. *Clin. Chim. Acta,* **350**, 129-136.

105. Giunta, S., Valli, M. B., Galeazzi, R., Fattoretti, P., Corder, E. H. & Galeazzi, L. (2005). Transthyretin inhibition of amyloid beta aggregation and toxicity. *Clin. Biochem.* **38**, 1112-1119.

106. Hong, W. K., Han, E. H., Kim, D. G., Ahn, J. Y., Park, J. S. & Han, B. G. (2007). Amyloid-beta-peptide reduces the expression level of mitochondrial cytochrome oxidase subunits. *Neurochem. Res.* **32**, 1483-1488.

107. Jayaraman, M., Kannayiram, G. & Rajadas, J. (2008). Amyloid toxicity in skeletal myoblasts: implications for inclusion-body myositis. *Arch. Biochem. Biophys.* **474**, 15-21.

108. Mattson, M. P., Begley, J. G., Mark, R. J. & Furukawa, K. (1997). Abeta25-35 induces rapid lysis of red blood cells: contrast with Abeta1-42 and examination of underlying mechanisms. *Brain Res.* **771**, 147-153.

109. Schaeffer, V., Meyer, L., Patte-Mensah, C., Eckert, A. & Mensah-Nyagan, A. G. (2008). Dose-dependent and sequence-sensitive effects of amyloid-beta peptide on neurosteroidogenesis in human neuroblastoma cells. *Neurochem. Int.* **52**, 948-955.

110. Xu, H., Wang, H., Zhuang, L., Yan, B., Yu, Y., Wei, Z., Zhang, Y., Dyck, L. E., Richardson, S. J., He, J., Li, X., Kong, J. & Li, X. M. (2008). Demonstration of an anti-oxidative stress mechanism of quetiapine: implications for the treatment of Alzheimer's disease. *FEBS J.* **275**, 3718-3728.

111. Khurana, R., Coleman, C., Ionescu-Zanetti, C., Carter, S. A., Krishna, V., Grover, R. K., Roy, R. & Singh, S. (2005). Mechanism of thioflavin T binding to amyloid fibrils. *J. Struct. Biol.* **151**, 229-238.

112. LeVine, H., 3rd. (1993). Thioflavine T interaction with synthetic Alzheimer's disease beta-amyloid peptides: detection of amyloid aggregation in solution. *Protein Sci.* **2**, 404-410.

113. LeVine, H., 3rd. (1995). Thioflavine T interaction with amyloid beta-sheet structures. *Amyloid: Int. J. Exp. Clin. Invest.* **2**, 1-6.

114. LeVine, H., 3rd. (1999). Quantification of beta-sheet amyloid fibril structures with thioflavin T. *Methods Enzymol.* **309**, 274-284.

115. Naiki, H., Higuchi, K., Hosokawa, M. & Takeda, T. (1989). Fluorometric determination of amyloid fibrils in vitro using the fluorescent dye, thioflavin T1. *Anal. Biochem.* **177**, 244-249.

116. Nilsson, M. R. (2004). Techniques to study amyloid fibril formation in vitro. *Methods,* **34**, 151-160.

117. Orte, A., Birkett, N. R., Clarke, R. W., Devlin, G. L., Dobson, C. M. & Klenerman, D. (2008). Direct characterization of amyloidogenic oligomers by single-molecule fluorescence. *Proc. Natl. Acad. Sci. USA,* **105**, 14424-14429.

118. Eisenberg, D., Nelson, R., Sawaya, M. R., Balbirnie, M., Sambashivan, S., Ivanova, M. I., Madsen, A. O. & Riekel, C. (2006). The structural biology of protein aggregation diseases: fundamental questions and some answers. *Acc. Chem. Res.* **39**, 568-575.

119. Ippel, J. H., Olofsson, A., Schleucher, J., Lundgren, E. & Wijmenga, S. S. (2002). Probing solvent accessibility of amyloid fibrils by solution NMR spectroscopy. *Proc. Natl. Acad. Sci. USA,* **99**, 8648-8653.

120. Pike, C. J., Overman, M. J. & Cotman, C. W. (1995). Amino-terminal deletions enhance aggregation of beta-amyloid peptides in vitro. *J. Biol. Chem.* **270**, 23895-23898.

121. de Groot, N. S., Aviles, F. X., Vendrell, J. & Ventura, S. (2006). Mutagenesis of the central hydrophobic cluster in Abeta42 Alzheimer's peptide. Side-chain properties correlate with aggregation propensities. *FEBS J.* **273**, 658-668.

122. Abedini, A. & Raleigh, D. P. (2006). Destabilization of human IAPP amyloid fibrils by proline mutations outside of the putative amyloidogenic domain: is there a critical amyloidogenic domain in human IAPP? *J. Mol. Biol.* **355**, 274-281.

123. Yamaguchi, K., Katou, H., Hoshino, M., Hasegawa, K., Naiki, H. & Goto, Y. (2004). Core and heterogeneity of beta2-microglobulin amyloid fibrils as revealed by H/D exchange. *J. Mol. Biol.* **338**, 559-571.

124. Frare, E., Mossuto, M. F., Polverino de Laureto, P., Dumoulin, M., Dobson, C. M. & Fontana, A. (2006). Identification of the core structure of lysozyme amyloid fibrils by proteolysis. *J. Mol. Biol.* **361**, 551-561.

125. Monti, M., Amoresano, A., Giorgetti, S., Bellotti, V. & Pucci, P. (2005). Limited proteolysis in the investigation of beta2-microglobulin amyloidogenic and fibrillar states. *Biochim. Biophys. Acta,* **1753**, 44-50.

126. Madine, J., Doig, A. J. & Middleton, D. A. (2008). Design of an N-methylated peptide inhibitor of alpha-synuclein aggregation guided by solid-state NMR. *J. Am. Chem. Soc.* **130**, 7873-7881.

127. Bitan, G., Kirkitadze, M. D., Lomakin, A., Vollers, S. S., Benedek, G. B. & Teplow, D. B. (2003). Amyloid beta -protein (Abeta) assembly: Abeta 40 and Abeta 42 oligomerize through distinct pathways. *Proc. Natl. Acad. Sci. USA,* **100**, 330-335.

128. El Moustaine, D., Perrier, V., Smeller, L., Lange, R. & Torrent, J. (2008). Full-length prion protein aggregates to amyloid fibrils and spherical particles by distinct pathways. *FEBS J.* **275**, 2021-2031.

129. Komatsu, H., Shinotani, N., Kimori, Y., Tokuoka, J., Kaseda, K., Nakagawa, H. & Kodama, T. (2006). Aggregation of partially unfolded Myosin subfragment-1

into spherical oligomers with amyloid-like dye-binding properties. *J. Biochem.* **139**, 989-996.

130. Martins, S. M., Frosoni, D. J., Martinez, A. M., De Felice, F. G. & Ferreira, S. T. (2006). Formation of soluble oligomers and amyloid fibrils with physical properties of the scrapie isoform of the prion protein from the C-terminal domain of recombinant murine prion protein mPrP-(121-231). *J. Biol. Chem.* **281**, 26121-26128.

131. Plakoutsi, G., Bemporad, F., Calamai, M., Taddei, N., Dobson, C. M. & Chiti, F. (2005). Evidence for a mechanism of amyloid formation involving molecular reorganisation within native-like precursor aggregates. *J. Mol. Biol.* **351**, 910-922.

132. Qi, W., Zhang, A., Patel, D., Lee, S., Harrington, J. L., Zhao, L., Schaefer, D., Good, T. A. & Fernandez, E. J. (2008). Simultaneous monitoring of peptide aggregate distributions, structure, and kinetics using amide hydrogen exchange: application to Abeta(1-40) fibrillogenesis. *Biotechnol. Bioeng.* **100**, 1214-1227.

133. Kayed, R., Pensalfini, A., Margol, L., Sokolov, Y., Sarsoza, F., Head, E., Hall, J. & Glabe, C. (2009). Annular protofibrils are a structurally and functionally distinct type of amyloid oligomer. *J. Biol. Chem.* **284**, 4230-4237.

134. Kumar, S. & Udgaonkar, J. B. (2009). Conformational conversion may precede or follow aggregate elongation on alternative pathways of amyloid protofibril formation. *J. Mol. Biol.* **385**, 1266-1276.

135. Hartley, D. M., Walsh, D. M., Ye, C. P., Diehl, T., Vasquez, S., Vassilev, P. M., Teplow, D. B. & Selkoe, D. J. (1999). Protofibrillar intermediates of amyloid beta-protein induce acute electrophysiological changes and progressive neurotoxicity in cortical neurons. *J. Neurosci.* **19**, 8876-8884.

136. Patel, N. S., Quadros, A., Brem, S., Wotoczek-Obadia, M., Mathura, V. S., Laporte, V., Mullan, M. & Paris, D. (2008). Potent anti-angiogenic motifs within the Alzheimer beta-amyloid peptide. *Amyloid,* **15**, 5-19.

137. Yagi, H., Sato, A., Yoshida, A., Hattori, Y., Hara, M., Shimamura, J., Sakane, I., Hongo, K., Mizobata, T. & Kawata, Y. (2008). Fibril formation of hsp10 homologue proteins and determination of fibril core regions: differences in fibril core regions dependent on subtle differences in amino acid sequence. *J. Mol. Biol.* **377**, 1593-1606.

138. Dobson, C. M. (1999). Protein misfolding, evolution and disease. *Trends Biochem. Sci.* **24**, 329-332.

139. Dobson, C. M. (2003). Protein folding and misfolding. *Nature,* **426**, 884-890.

140. Fandrich, M. & Dobson, C. M. (2002). The behaviour of polyamino acids reveals an inverse side chain effect in amyloid structure formation. *EMBO J.* **21**, 5682-5690.

141. Street, A. G. & Mayo, S. L. (1999). Intrinsic beta-sheet propensities result from van der Waals interactions between side chains and the local backbone. *Proc. Natl. Acad. Sci. USA,* **96**, 9074-9076.

142. Sato, K., Wakamiya, A., Maeda, T., Noguchi, K., Takashima, A. & Imahori, K. (1995). Correlation among secondary structure, amyloid precursor protein accumulation, and neurotoxicity of amyloid beta(25-35) peptide as analyzed by single alanine substitution. *J. Biochem.* **118**, 1108-1111.

143. Meinhardt, J., Sachse, C., Hortschansky, P., Grigorieff, N. & Fandrich, M. (2009). Abeta(1-40) fibril polymorphism implies diverse interaction patterns in amyloid fibrils. *J. Mol. Biol.* **386**, 869-877.

144. Makarava, N., Ostapchenko, V. G., Savtchenko, R. & Baskakov, I. V. (2009). Conformational switching within individual amyloid fibrils. *J. Biol. Chem.* **284**, 14386-14395.

145. Tycko, R., Sciarretta, K. L., Orgel, J. P. & Meredith, S. C. (2009). Evidence for novel beta-sheet structures in Iowa mutant beta-amyloid fibrils. *Biochemistry,* **48**, 6072-6084.

VITA

Name:	Katherine Vale Ridinger
Address:	c/o Dr. J. Martin Scholtz 440 Reynolds Medical Building 1114 TAMU College Station, TX 77843-1114
Email Address:	kriding@tamu.edu
Education:	B.S., Biochemistry, Angelo State University, 2004 Ph.D., Biochemistry, Texas A&M University, 2009